

STUDIES ON THE ENZYMOLOGY OF STEROL METHYL

TRANSFERASE FROM Saccharomyces cerevisiae

by

JULIE A. MARSHALL, B.S.Ed., M.S.

A DISSERTATION

IN

CHEMISTRY

Submitted to the Graduate Faculty
of Texas Tech University in
Partial Fulfillment of
the Requirements for
the Degree of

DOCTOR OF PHILOSOPHY

Approved

Chairperson of the Committee

Accepted

Interim Dean of the Graduate School

May, 2001

ACKNOWLEDGEMENTS

I would like to thank the following people for their help and support during the research and writing of my thesis: Dr. W. David Nes for mentoring and advising me; the Nes lab members, specifically Wen-xu Zhou, Anil Mangla, Allen Dennis, Ann Marie Haynes, and Dr. Haoxia Li. The support of the Welch Foundation, the THECB-Advanced Technology Program, and the ARCS Foundation is gratefully acknowledged.

I would also like to thank my family for their patience and support of me during my doctoral work.

TABLE OF CONTENTS

ACKNOWLEDGEMENTS	ii
ABSTRACT	v
LIST OF TABLES	vi
LIST OF FIGURES	vii
LIST OF ABBREVIATIONS	x
CHAPTER	
I. STEROL METHYL TRANSFERASE (SMT) ENZYME AND MECHANISM OF METHYLATION	1
Description of the SMT Enzyme from <i>Saccharomyces cerevisiae</i>	1
History and Mechanism of Methylation	2
Alkylation-Reduction Bifurcation	3
Mechanism of Methylation	3
Research Aims	6
II. EXPERIMENTAL METHODS	14
Preparation of the Sterol Methyl Transferase	14
Assay Protocol and Formulas	16
Tryptic Digest Protocol	19
Site-Directed Mutagenesis	20
Photolabeling of the SMT with AdoMet	21
Western Blotting	22
Purification of the Antibody	24

	Equilibrium Dialysis Experiments and Determination of Binding Constants	24
III.	ALLOSTERIC MODULATION OF THE STEROL METHYL TRANSFERASE ENZYME	30
	Allosteric Modulation by ATP	30
	Kinetic Studies with the Native Recombinant SMT	31
	Kinetic Studies with the Y81F Mutant SMT	32
	Kinetic Studies with <i>Arabidopsis thaliana</i>	33
IV.	KINETIC AND THERMODYNAMIC CONTROL OF SUBSTRATE-ENZYMES INTERACTIONS	42
	SMT Substrate Specificity	42
	Protein-Ligand Binding Equilibria	44
	Equilibrium Studies on the Native Substrates	46
	Equilibrium Studies on Other Sterols	47
	Gibb's Free Energy of Binding	48
V.	ACTIVE SITE MAPPING	57
	Affinity Labeling of the SMT Sterol Binding Site	57
	Affinity Labeling of the AdoMet Binding Site	59
	Site Specific Mutagenesis of Regions I and II	61
VI.	SITE SPECIFIC MUTAGENESIS OF TYROSINE 81	78
	Kinetic Isotope Effects	78
	Equilibrium Dialysis and Kinetic Experiments	80
VII.	DISCUSSION	90
	SELECTED BIBLIOGRAPHY	93

ABSTRACT

As an approach to understanding the enzymological details of sterol methylation catalysis in ergosterol biosynthesis, a kinetic analysis as well as an active site mapping study of the active center of the sterol methyl transferase (SMT) was pursued using a recombinant SMT from *Saccharomyces cerevisiae*. The following experiments were performed:

- i. Using initial velocity conditions and equilibrium dialysis to establish the kinetic constants, K_m , V_{max} , and K_d , respectively, the kinetic behavior of the native SMT and a set of site-specific mutants corresponding to either the sterol or AdoMet binding site was established.
- ii. Using native and mutant SMTs that exhibit differences in the complement of C_1/C_2 -activities the modulation of SMT activity by effectors such as ATP and ergosterol was determined.
- iii. Photoaffinity labeling of the active site using [3H_3 -methyl] AdoMet and site-specific mutagenesis experiments were designed which successfully led to the identification of the AdoMet binding site on the SMT.

The results of these studies and that of other studies from this laboratory involving the active site characterization of the sterol binding domain, are interpreted to imply that the SMT contains an active center in which there is a sterol and AdoMet binding motif spatially disposed to allow for a random bi bi kinetic mechanism in C -methylation of a sterol acceptor molecule. A second distinct binding center on the SMT is considered for modulators.

LIST OF TABLES

2.1	Quantification of the yeast SMT	28
2.2	Oligonucleotide primers synthesized for mutagenesis and sequencing	29
3.1	Kinetic parameters for substrates of the yeast SMT	41
4.1	Steps in the purification for the recombinant yeast SMT	55
4.2	Dissociation constants and calculated Gibb's free energy	56
5.1	Equilibrium binding constants and catalytic competence for the native SMT and 3 selected mutants from Regions I and II	77
6.1	Kinetic and equilibrium dialysis results for the native SMT and Y81 series with zymosterol and 26,27-dehydrozymosterol	89

LIST OF FIGURES

1.1	The alkylation/reduction bifurcation	9
1.2	Fungal and plant pathways for C-methylation reactions	10
1.3	The two proposed mechanisms of methylation for the SMT enzyme	11
1.4	The steric-electric plug model	12
1.5	The four domains of the sterol molecule	13
2.1	Substrates and inhibitors of the yeast SMT enzyme	26
2.2	Preparation of 3-tritio Δ^8 sterols	27
3.1	Amino acid composition of the proposed ATP binding site aligned against the sequences of related SMTs	34
3.2	The structure of Adenosine Triphosphate	35
3.3	Variations in the activity of the native SMT with 50 μM zymosterol and increasing ATP concentration	36
3.4	Inhibition plot for the native SMT with 50 mM zymosterol and increasing ergosterol in the presence of 0.4 mM ATP	37
3.5	Binding isotherm for the native SMT in the presence of increasing ATP concentration	38
3.6	Lineweaver-Burke plot of SMT activity with and without ATP	39
3.7	Variations in the activity of the mutant Y81F SMT with 50 μM fecosterol, 50 μM zymosterol and increasing ATP concentration	40
4.1	Binding isotherm for the native SMT in the presence of increasing zymosterol concentration	50
4.2	Binding isotherm for the native SMT in the presence of increasing AdoMet concentration	51
4.3	Sterol substrates of the yeast SMT with structural features highlighted	52

4.4	Binding isotherm for the native SMT in the presence of increasing lanosterol concentration	53
4.5	Binding isotherm for the native SMT in the presence of increasing 24-epiminolanosterol concentration	54
5.1	The structure of 26,27-dehydrozymosterol	63
5.2	The proposed mechanism of inactivation of the SMT enzyme by 26,27-dehydrozymosterol	64
5.3	Time dependent inactivation of the yeast SMT with DHZ	65
5.4	SDS-PAGE and corresponding film of the SMT-DHZ adduct	66
5.5	Amino acid composition of Region I from several SMTs	67
5.6	Radioactive counts of individual fractions corresponding to the amino acid residues sequenced in Region I	68
5.7	Theoretical model of the yeast SMT active site pictured with the co-substrates, ergosterol and AdoMet	69
5.8	Percent SMT activity remaining versus time of UV irradiation of SMT and AdoMet at 254 nm	70
5.9	SDS-PAGE and corresponding film of the SMT-AdoMet adduct	71
5.9	Radioactive counts of the fractions collected from the HPLC purification of the complexed SMT-AdoMet tryptic peptides versus time of fraction collection	72
5.11	Amino acid composition of Region II from several SMTs	73
5.12	MALDI-TOF analysis of the tryptic digested AdoMet-SMT complex	74
5.13	Amino acid substitutions in the site-specific mutagenesis of Regions I and II	75
5.14	The Western blot of the T78V and P133L mutant SMTs	76
6.1	Amino acid substitutions in the site-specific mutagenesis of tyrosine 81	77
6.2	MALDI-TOF analysis of the Y81F mutant SMT	82

6.3	MALDI-TOF analysis of the Y81W mutant SMT	83
6.4	Western blot of the yeast mutant Y81 SMTs	84
6.5	Inhibition plot of Y81W mutant SMT with 50 μ M zymosterol and increasing DHZ	85
6.6	Inhibition plot of Y81F mutant SMT with 50 μ M zymosterol and increasing DHZ	86
6.7	Inhibition plot of Y81L mutant SMT with 50 μ M zymosterol and increasing DHZ	87
6.8	Time dependent inactivation of the Y81W mutant SMT with DHZ	88

LIST OF ABBREVIATIONS

SMT- sterol methyl transferase

AdoMet- (S)-adenosyl-L-methionine

IPTG- isopropyl- β -D-thiogalactoside

SDS-PAGE- sodium dodecyl sulfate polyacrylamide gel electrophoresis

HPLC- high performance liquid chromatography

GLC- gas liquid chromatography

DHZ- 26,27-dehydrozymosterol

BSA- bovine serum albumin

TBS- tris-buffered saline

ATP- adenosine triphosphate

IC₅₀- inhibitor concentration at 50% activity

[]- bracketed compound is operationally defined to mean concentration of that compound

PCR- polymerase chain reaction

DNA- deoxyribose nucleic acids

CHAPTER I
STEROL METHYL TRANSFERASE ENZYME AND
MECHANISM OF METHYLATION

Description of the SMT Enzyme from
Saccharomyces cerevisiae

Sterol biosynthesis is one of the few areas of difference in primary metabolism in the plant and animal kingdoms including the fungi. Animals synthesize C₂₇ cholestane-based members of the steroid family, whereas plants synthesize C₂₈ and C₂₉ compounds in which an extra methyl or ethyl group is added to carbon-24 of the sterol side chain (Nes and McKean, 1977). The enzyme responsible for the addition of a methyl group to carbon-24 is the sterol methyl transferase (SMT). (S)-Adenosyl-L-methionine (AdoMet) linked biological methylations of sterols and other natural products represent about 3% of 3196 known enzymes (Nes et al., 1998). The apparent similarities between the transfer mechanisms of methyls to sterols suggest quaternary structure and specialized structure likenesses between them. However, the ability of certain methyl transferases to catalyze two methylations suggests the topology of the active site of the enzymes contains marked differences.

In the past five years, there have been several advances in the study of SMT enzymes. First, a recombinant SMT from *Saccharomyces cerevisiae* has been overexpressed in *Escherichia coli* in large amounts to permit detailed kinetic and structural analyses (Nes et al., 1998). Second, at least 19 different sequences of SMTs from 16 species of plants and fungi have been reported in the GenBank and the structures

of 9 related AdoMet-dependent methyl transferases have been solved (Niewmierzycka and Clarke, 1999). In the three-dimensional structures of these proteins a similar folding pattern with the central parallel β -sheet surrounded by α -helices is observed. The common three-dimensional structure of AdoMet-dependent enzymes is reflected further in sequence motifs that are conserved among a large number of AdoMet-dependent methyl transferases, including SMTs (Kagan and Clarke, 1994). Third, several potent SMT inhibitors were tested including a new class of mechanism-based irreversible enzyme inactivators (Marshall and Nes, 1999). These inhibitors, acting as substrate analogs and in chemical affinity labeling of the active site of the SMTs, have provided detailed information about the active site topography in the absence of structural information about the three-dimensional architecture of the enzyme. Finally, it was demonstrated for the first time that a single substitution in the primary sequence can lead to a dramatic change in the sterol specificity, product distribution and degree of consecutive C-methylations performed by the enzyme (Nes et al., 1999). This observation can have significant consequences in relation to rational drug design and to the molecular engineering of the phytosterol pathway.

History and Mechanism of Methylation

In most organisms, the dominant sterols possess the following characteristics: Δ^5 -bond, no carbon substituents on C-4 or C-14, a methyl group on the A/B ring juncture, and the absence of a three-membered 9,19 cyclo group (Nes and McKean, 1977). Since lanosterol and cycloartenol do not possess these characteristics there must be a process

for the formation of products including the Δ^5 -double bond introduction, demethylation at C-4 and C-14, an opening of the 9,19 cyclo ring (cycloartenol), and Δ^{24} metabolism. In addition, there seems to be an order in the way these changes are accomplished. The metabolism at C-24 is the major step known as the alkylation-reduction bifurcation.

Alkylation-Reduction Bifurcation

Metabolism at C-24 is a source of diversity in Δ^5 sterols in plants and animals (Parker and Nes, 1992). The route of metabolism proceeds through either alkylation or reduction at C-24 (Figure 1.1, Parker and Nes, 1992). Thus the double bond at C-24(25) is either alkylated or reduced. There are mechanistic similarities in the path of either event. Malhotra and Nes (1971) studied the reaction and found that the stereochemistry of C-24 is directly related to the distribution of sterol products. The methylation event itself results in a particular stereochemistry at this position. The methylation is governed by kinetic control and follows an alkylation pathway which gives rise to $\Delta^{24(28)}$ -sterols.

Mechanism of Methylation

The methyl group attached to the sterol side chain at C-24 proceeds by the formation of a 24-methyl carbonium ion intermediate at C-25 (Nes, 2000). The carbonium ion obtained by the alkylation can undergo several reactions: (a) proton elimination and formation of a double bond, (b) cyclization to form a cyclopropyl system with the elimination of a proton and (c) quenching to form a saturated side chain. Carbocations typical of those generated during biomimetic C-methyl transfer reactions of

an olefin are notoriously unselective in their reactions (Julia and Marazano, 1985). The enzyme could, in theory, capitalize on this low selectivity to generate a variety of structures. The enzyme-substrate interactions specific to the fungal SMT were related to the formation of a 24 β -methyl intermediate (Figure 1.2). The resulting 24(28)-methylene product possesses a C-25 hydrogen which is generated during the methylation reaction by H-24 migrating to C-25 from the *Si*-face of the original substrate double bond.

How SMTs generate the C-25 stereochemistry and by analogy the steric course of C-methylation of the substrate double bond has only recently been debated. Two opposing mechanistic schemes for C-methylation of sterol are illustrated in Figure 1.3 (Nes, 2000). According to the covalent mechanism (path a, X⁻group mechanism), the reaction of zymosterol is initiated by the enzyme-catalyzed attack of the π -electrons associated with the Δ^{24} -bond on the methyl carbon of AdoMet that is assisted by a counter ion to AdoMet that becomes the deprotonating agent used to capture a hydrogen from C-28. The reaction has stereochemical consequences; the nucleophilic substitution mechanism will be, inversion, retention or racemization at the transferring chiral methyl center. The purpose of employing an “X⁻group” mechanism in SMT catalysis (Wokciechowski, Goad, and Goodwin, 1973) was believed to control the stereochemistry at C-25 during C-methylation of the substrate double bond in order to produce the natural configuration of 25*R*. Addition of the methyl group to the *Re*-face of the substrate double bond and concomitant antiperiplanar addition of an X⁻group would give a covalently bound intermediate.

A new model, the steric-electric plug model (Figure 1.4), proposed by Parker and Nes (1992) for the C-methyl transfer reaction idealized a concerted mechanism with the substrate furnishing only one enantiomer. In the non-covalent pathway (path b, Figure 1.3), the C-methyl transfer reaction occurs via a S_N2 type mechanism of C-methyl attachment to the Δ²⁴-bond from its backside (β-face). Additionally, specific sterol features, particularly, a free equatorial C-3 hydroxyl, a flat molecule, and the side chain to extend into a “right-handed” and pseudocyclic side chain conformation for productive binding of the substrate to the enzyme. In 1978, Arigoni studied the yeast SMT reporting that the catalyzed reaction proceeds with inversion of configuration of the incoming methyl from AdoMet to C-24 rules out a stepwise mechanism but is consistent with other possibilities. Additional kinetic and mechanistic studies in the Nes laboratory (Nes et al., 1998; Venkatramesh, Guo, Jia, and Nes, 1996) have produced evidence which appears to exclude covalent participation of a nucleophile X⁻ group in the active site while indicating a random bi bi mechanism whereby a rigidly held bridged carbenium ion intermediate gives rise to a nucleophilic rearrangement in which H-24 migrates to C-25 on the *Re*-face of the substrate double bond in concert with the initial ionization. Kinetic studies showing an unhindered C-3 hydroxyl group and a specific spatial arrangement of the substrate double bond undergoing C-methylation are essential for substrate-enzyme interactions hold the key to the generation of specific chirality at C-25 during fecosterol synthesis.

The results from these previous studies are indicated in Figure 1.4. When the substrate double bond interacts with the SMT enzyme, the isopropyl group in the side

chain should be oriented so that the *Si*-face of the 24,25-double bond is opposite to the methyl group projecting axially from AdoMet. The positioning and relative charges from the sulfur of AdoMet and the π -lobe of the double bond facilitate the *C*-methyl transfer reaction stereoselectively with an S_N2 inversion occurring at the C-24 center. The steric-electric plug model incorporates a two-base system. In the case of the yeast SMT, one base is hypothesized to assist in anchoring zymosterol into the enzyme-substrate complex via hydrogen bonding interactions with the C-3 hydroxyl group and a second base contributes to the *C*-methyl transfer reaction by serving as a deprotonating agent to remove the hydrogen at C-28 in fecosterol synthesis. The nature of these bases has been considered. For instance, the hydroxyl group of the sterol can be in proximity to a tyrosine residue (Nes et al., 1999). A sterol carrier protein from the *Phytophthora* fungi has been crystallized and the C-3 hydroxyl group of ergosterol was found to be interacting with a tyrosine residue in the sterol binding site (Boissy et al., 1999). The identity of the second base has been hypothesized to be a carboxylate anion that can also interact as a counterion to AdoMet in the active site (Rahier, Genol, Schuber, Benveniste, and Narula, 1984).

Research Aims

The differences in methylation mechanism described in the previous sections raise several questions; first, what features of the sterol are required for binding and/or catalysis; second, what regions of the protein constitute the active site and which amino acid residues have special significance in the reaction mechanism; and third, what

allosteric conditions influence enzyme activity. Therefore the major goal of this research project is to develop a fundamental understanding of the specificity, catalytic, and regulatory mechanisms, three-dimensional structures, including the active site domain of SMT enzymes involved in phytosterol biosynthesis as described in the specific aims to follow.

- Both kinetic and equilibrium binding constants will be determined for the SMT utilizing a variety of sterol substrates. At least 4 critical structural elements of recognition can be identified from the features associated with zymosterol (the preferred substrate of the yeast SMT): (1) C₃-OH group, (2) double bond position in the nucleus, (3) *R*-stereochemistry at C-20, and (4) the position of the Δ^{24} -bond in the side chain (Figure 1.5). Confirmation of sterol features required as “principle determinants” in binding will be demonstrated using steady-state analyses; K_m , V_{max} , and catalytic competence, as well as equilibrium binding constants, K_d .
- Allosteric effectors, both sterol and other metabolic activators, will be studied examining the effect of the compounds on steady-state kinetic parameters, equilibrium dialysis and product partitioning in the *C*-methylation pathway.
- From homology building regions of sequence conservation are indicated. Therefore, site-specific mutants related to these motifs will be generated. The resulting *C*-methyl products will be characterized to determine the role of key amino acid residues involved with binding and transformation of the phytosterol side chain to one or more olefins. Site-specific mutagenesis will be employed for

rational design of novel mutants. Mutant forms which retain some or all of the original activity can be characterized by a combination of equilibrium dialysis, steady-state kinetic analysis, MALDI-TOF and Western blotting.

- Several fragments of sequences from various organisms with high homology to SMT enzymes have been identified. Affinity labeling will identify regions of the SMT critical to catalytic activity. The AdoMet binding site will be determined via photolabeling of the SMT with AdoMet. Proteolytic digestion by trypsin will generate peptide fragments that have been covalently modified. The peptide adduct will be sequenced by Edman degradation to confirm the sequence corresponding to the highly conserved regions of the SMT hypothesized to be the active site.

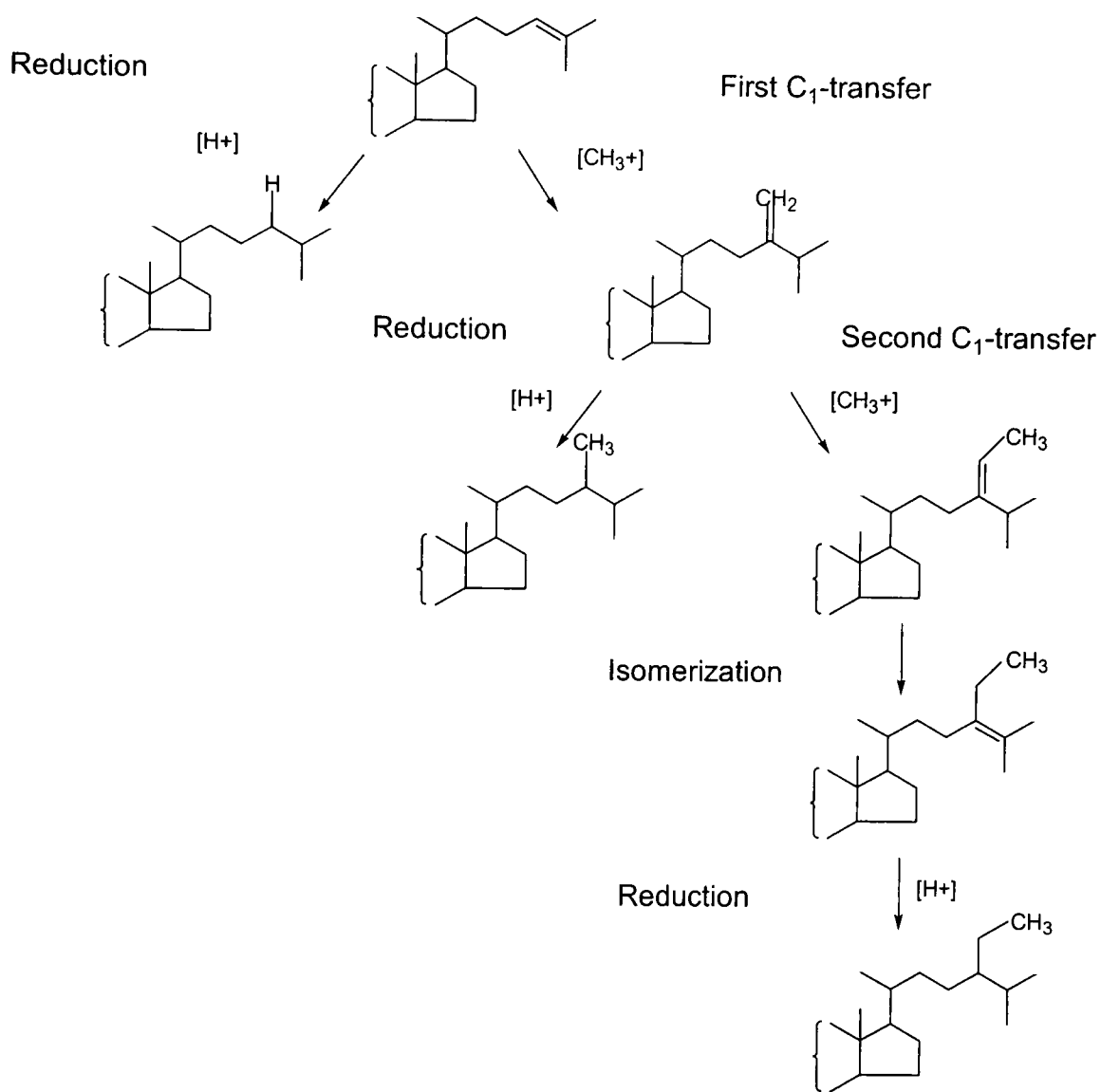


Figure 1.1. The alkylation/reduction bifurcation.

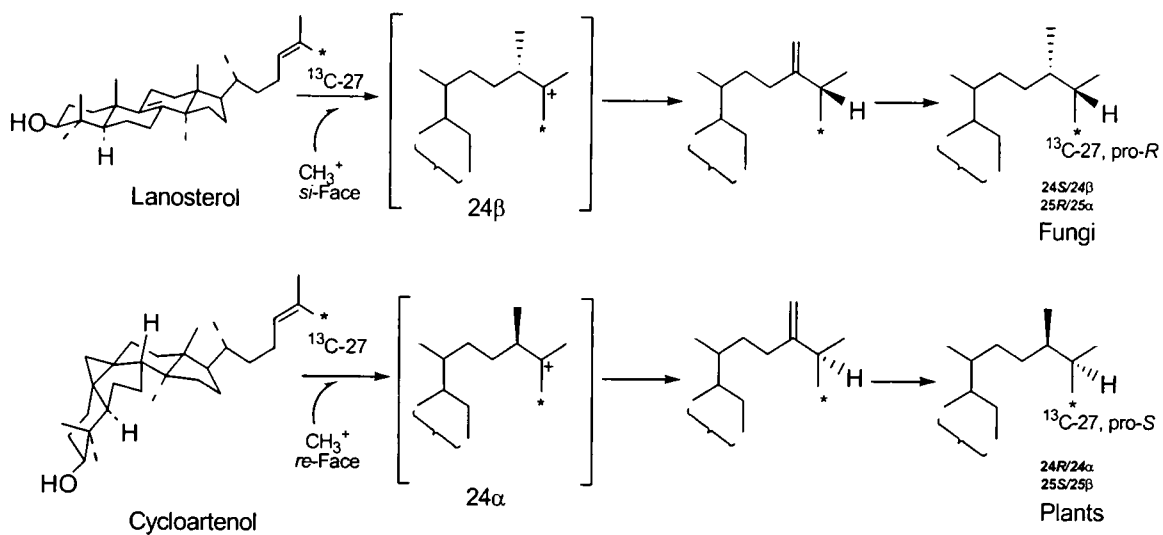


Figure 1.2. C-Methyl transfer reactions emphasizing the structures of the substrates affecting the stereochemistry of the products.

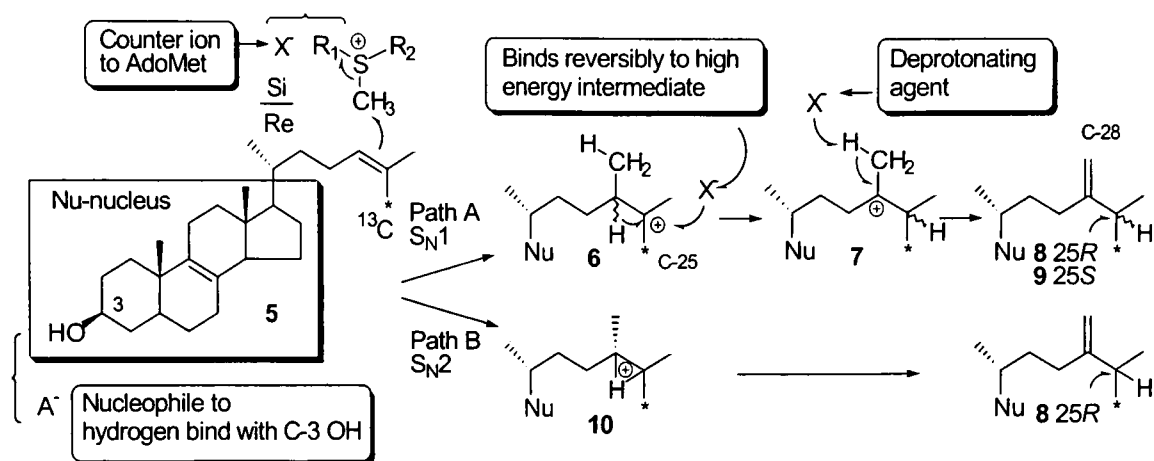


Figure 1.3. The two proposed mechanisms of methylation for the SMT enzyme. X^- and A^- represent different bases in the active center.

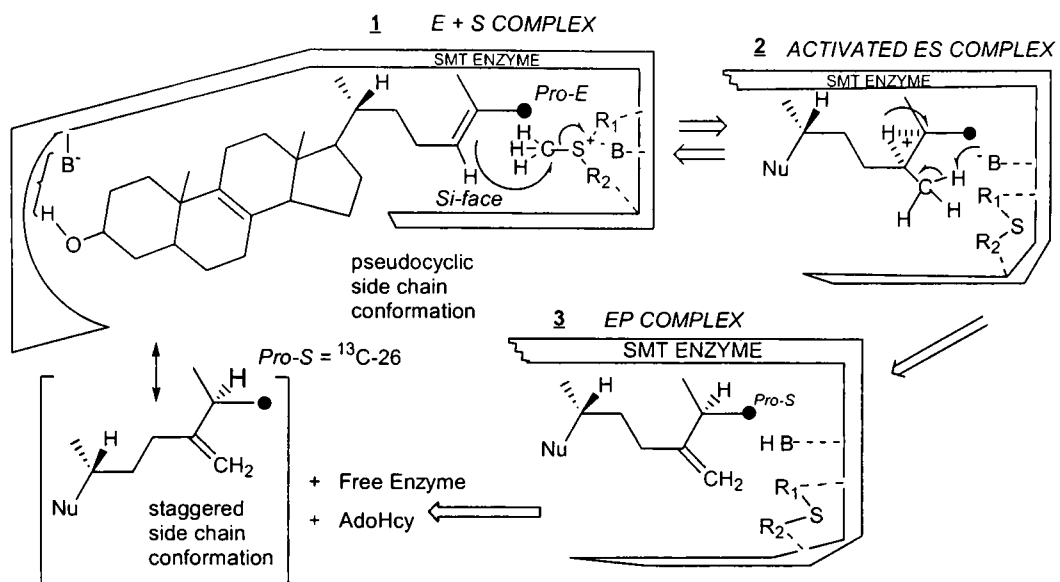


Figure 1.4. Steric-electric plug model.

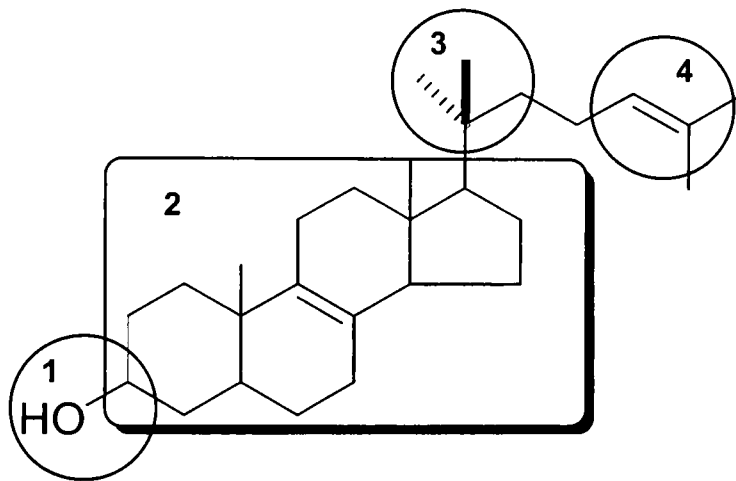


Figure 1.5. The four domains of the sterol molecule.

CHAPTER II

EXPERIMENTAL METHODS

Preparation of the Sterol Methyl Transferase

The SMT from yeast has been investigated as a cell-free protein. The enzyme is membrane-bound and it can distribute among different subcellular fractions, including the endoplasmic reticulum, mitochondria and a “floating lipid layer” (Zisner, Paltauf, and Daum, 1993). The SMT from yeast is synthesized in low abundance so that it is difficult to obtain large amount of the enzyme for purification as well as being somewhat unstable. The breakthrough in purification of SMT to homogeneity from any source was achieved in the Nes laboratory in 1998 using a recombinant yeast SMT (Nes et al., 1998). The *ERG6* gene which encodes SMT from *S. cerevisiae* was introduced into plasmid pET23a(+) and the resulting native protein was overexpressed in BL21(DE3) host cells under control of a T₇ promoter. The procedure which is used in the Nes group routinely to generate both native and mutant recombinant SMT is described in the following paragraphs.

A single colony of *E.coli* BL21(DE3) is transferred from a Luria broth agar plate with ampicillin (Difco bacto-tryptone 10 mg/ml, Difco bacto-yeast extract 5 mg/ml, NaCl 10 mg/ml, and agar 7.5 mg/ml, pH 7.0) to a fresh LBA plate. The ampicillin stock (50 mg/ml) is added to the media prior to the pouring of the plates. The inoculated plate is incubated for 16 hours at 37°C. The plate is directly used to prepare the starter culture. Using the freshly inoculated plate the starter culture is prepared. A single colony is

transferred into 200 ml of LB media that contains 200 μ l of the ampicillin stock. The mixture is incubated at 37°C and 250 rpm for 8-10 hours until an optical density of 1.0 is reached (600 nm, mid-logarithmic phase growth). Then 8, 25 ml, portions of cultured cells are inoculated into 8, 2.7 L, Fernbach flasks each containing 1 L of LB medium with 1.0 ml of ampicillin stock. The cultures are incubated at 37°C and 250 rpm until an optical density of 0.6 is reached (600 nm). IPTG (0.4 mM, 4 ml of an 100 mM stock solution) is added to each flask to induce the production of SMT, and the cultures are incubated at 37°C and 250 rpm for 2 hours. The cells are harvested by centrifugation at 10,000 x g for 10 minutes and either used immediately or stored at -20°C for up to 1 month.

All purification manipulations are carried out at 4°C on ice or in the Revco Commercial Refrigerator. The cell pellet that was harvested (about 25.0 g fresh weight) is thawed and resuspended in 180 ml of resuspension buffer containing: 50 mM Tris HCl; 2 mM magnesium chloride; 2 mM β -mercaptoethanol; and 5% glycerol (v/v); pH 7.5. The resuspended cells are disrupted by sonication using a sonifier (Model #250 Sonifier, Branson UltraSonocs Corp., Danbury, CT). The power is set at 7, duty cycle to 50% and sonify for 5 minutes, rest for 3 minutes, and repeat twice more. Then the mixture is centrifuged at 10,000 x g for 20 minutes and the supernatant collected. The supernatant is further centrifuged at 100,000 x g for one hour. The supernatant is collected and subjected to precipitation by 60% saturation with ammonium sulfate and stirred for 30 minutes on ice. The precipitated protein is pelleted by centrifugation at 100,000 x g for 30 minutes. The protein is desalted by resuspending the pellet in Q Sepharose buffer A

containing: 50 mM Tris HCl, pH 8.0; 2 mM magnesium chloride; 2 mM β -mercaptoethanol; 1 mM EDTA and 15% glycerol (v/v). Then the mixture is dialyzed at 4°C in molecularporous membrane tubing (Spectra/Por, 6 to 8 kDa, Spectrum Medical Ind., CA) for 12-16 hours with at least 1 buffer exchange.

After dialysis, the entire mixture is loaded onto the Q Sepharose column (2.5 x 15 cm) which is preequilibrated with Q Sepharose buffer A. The protein is eluted in a bimodal fashion. SMT elutes from the column following the void volume and aliquots of the desired fractions are located by activity and SDS-PAGE. Then the mixture is dialyzed against HIC buffer A containing: 50 mM MOPS, pH 6.5; 2 mM magnesium chloride; 2 mM β -mercaptoethanol; 1 mM EDTA and 15% glycerol (v/v). The enzyme solution is applied to an ω -aminodecyl agarose (hydrophobic interaction chromatography: HIC) column (2.5 x 7.5 cm) that is preequilibrated with 200 ml of HIC buffer A. The column is washed with 80 ml of buffer A, and eluted first with 200 ml of HIC buffer A then 200 ml of buffer B (1 M NaCl in HIC buffer A). The SMT will elute in the single peak in the first fractions eluting from the column. The SMT protein is now at least 90% pure as shown on SDS-PAGE and is suitable for kinetic and mapping procedures. The amount of protein is quantified by UV absorbance at 280 nm and concentration solved by the extinction coefficient for SMT (58,250 l/M*cm).

Assay Protocol and Formulas

A standard assay contains 600 μ l total volume with 2-3 mg of total protein in 50 mM Tris buffer, pH 7.5 (Nes et al., 1998). The substrate [*methyl*-³H] AdoMet is held at

50 μ M and the sterol substrate usually zymosterol is varied (Figure 2.1). The sterol substrate is added to the test tube containing Tween 80 (1% v/v) and then blown dry to aid in solubilizing the sterol. All protein samples are exchanged to Tris buffer via dilution, desalting, or dialysis prior to assaying. The assay mixture is incubated at 32°C for 45 minutes. The enzymatic reaction is stopped with 500 μ l of a solution containing 10 g of KOH dissolved in 10 ml of water and 90 ml of methanol. The methylated sterol product is extracted 3 times with 2.5 ml of skelly hexanes (Fisher) after mixing with a vortex mixer for 30 seconds. The organic layer is transferred to a 7 ml scintillation vial and then dried. The radioactive residue is resuspended in 5 ml of scintillation cocktail, vortexed, and then counted by scintillation.

All sterol substrates (Figure 2.1) were purified by recrystallization and high-performance liquid chromatography (HPLC) on a Whatman C18-reversed phase 25 cm column eluted with 9:1 isopropanol:acetonitrile with identification at 205 nm. All retention times are set relative to cholesterol. Quantification of substrates is performed on gas-liquid chromatography (GLC) 3% SE-30 packed column operated isothermally 240 °C with flame ionization detection (Nes et al., 1998). The 26,27-dehydrozymosterol (DHZ) was synthesized as described in Nes, Guo, and Zhou (1997) and labeled according to the method described in Nes and Le (1986, Figure 2.2). AdoMet is purchased from Sigma.

The structures of the four primary substrates and their respective molecular weights are shown in Figure 2.1. The molar amounts are based on the following calculation:

$$5.0 \times 10^{-5} \text{ mol/l} = 5.0 \times 10^{-8} \text{ mol/ml} = 5.0 \times 10^{-11} \text{ mol/}\mu\text{l} = 50 \mu\text{M}$$

$$5.0 \times 10^{-11} \text{ mol/}\mu\text{l} = x/600 \mu\text{l} = 3.0 \times 10^{-8} \text{ mol}$$

$$\text{AdoMet: } 3.0 \times 10^{-8} \text{ mol} \times 399 \text{ g/mol} = 11.97 \mu\text{g}$$

$$\text{Zymosterol : } 3.0 \times 10^{-8} \text{ mol} \times 384 \text{ g/mol} = 11.52 \mu\text{g}$$

$$26,27\text{-Dehydrozymosterol: } 3.0 \times 10^{-8} \text{ mol} \times 424 \text{ g/mol} = 12.72 \mu\text{g}.$$

After purification the sterol is resuspended in a suitable solvent such as ethanol. However, the exact concentration is not known and thus the correct amount of substrate for each assay cannot be added. To determine the proper amount of sterol, an aliquot of the sterol and one of standard cholesterol (1mg/ml) is taken and injected on the GLC. The retention areas for both substances is obtained and the amount of sterol is calculated in the following manner:

$$\text{Area sterol substrate/area cholesterol} = \# \text{ mg/ml}$$

$$50 \mu\text{M Zymosterol, } 11.52 \mu\text{g} \times 1 \text{ ml}/\# \text{ mg} \times 1 \text{ mg}/10^3 \mu\text{g} \times 10^3 \mu\text{l}/1 \text{ ml} =$$

volume of substrate for the assay.

The amount of SMT must also be known exactly to determine specific activity for the enzymatic system (pmol/min/mg protein). Protein can be quantified by a variety of methods with differing accuracy. An experiment was done to determine the accuracy of 3 commonly used methods. Duplicate samples of pure SMT were obtained and desalted by washing through Amicon Y30 concentrators with 2 times the volume of water. The protein was then lyophilized and quantified 3 different ways. First, an aliquot was run on SDS-PAGE and concentration estimated by using a standard of known concentration (Promega mid-range marker, Laemmli, 1970). Next, the Bradford method (1976) using

bovine serum albumin was performed measuring absorbance at 595 nm (BioRad protein assay). The BSA absorbencies were then plotted over the concentration range of 0 to 100 μg per μl . The absorbance of SMT at 595 nm was then taken and the result fitted to the standard curve and concentration solved. The third method was to measure the absorbance of SMT by UV scan (240 to 370 nm) and solving for concentration using the extinction coefficient for SMT. The extinction coefficient can then be used to find concentration according to Beer-Lambert's Law. The equations are as follows:

$$\epsilon, \text{ molar extinction coefficient} = \Sigma[n(\text{tyr}) \times 1280, n(\text{trp}) \times 5200, n(\text{s-s}) \times 120]$$

$$\epsilon, \text{ SMT} = 58,250/M*\text{cm}$$

$$\text{Concentration} = \text{absorbance}/\text{path length}*\epsilon$$

(*- multiplication by).

The percent error was calculated assuming the mass of lyophilized SMT to be correct. The error can be used as a correction factor to solve concentration for each method. The results are shown in Table 2.1.

Tryptic Digest Protocol

The SMT is first purified to homogeneity as previously described and either labeled with tritiated sterol (Marshall and Nes, 1999) or photo labeled (experimental details to follow). The procedure for digestion follows that highlighted in Methods for Protein Analysis (Copeland, 1994). The labeled enzyme complex is diluted to a 5-10 mg/ml concentration in buffer containing 8 M urea and 0.5 M ammonium bicarbonate, pH 8.0. The mixture is then flushed with nitrogen and incubated for 30 minutes at 37°C.

Next, 5 mM of β -mercaptoethanol is added and the mixture is flushed with nitrogen and incubated for 4 hours at 37°C. The solution is cooled on ice to 4°C. Iodoacetic acid (100 mM) is added and the pH adjusted back to 8.0 if necessary by adding the ammonium bicarbonate buffer. The protein solution is then incubated in the dark at room temperature for 15 minutes. After incubation, another 5 mM of β -mercaptoethanol is added to the solution. The mixture is concentrated through Amicon Y30 concentrators until the denaturants are removed. Next, the solution is boiled for 5 minutes to ensure that the protein is completely unfolded.

The trypsin is freshly prepared before each use by quickly thawing the lyophilized protein and resuspending in 200 μ l of resuspension buffer per each 20 μ g of trypsin. The trypsin should be 1-2% of the total protein content. The pH of the trypsin solution is measured and equilibrated to a pH of 8.0 with the ammonium bicarbonate buffer. The trypsin is then added to the denatured SMT and the entire mixture is incubated for 4-6 hours at 37°C. After the incubation is complete, the protein mixture is quickly frozen in liquid nitrogen to prevent the over degradation of either the SMT or trypsin. The tryptic digest is analyzed on SDS-PAGE and the desired bands can be cut out of the gel and eluted or transferred to nitrocellulose membrane for analysis. The gel can also be dried and exposed to film for 2 weeks for identification of labeled protein.

Site-Directed Mutagenesis

The *ERG6* gene that has been cloned and overexpressed in BL21(DE3) cells was used as the template for all mutagenesis reactions. Mutant primers and the sequencing

primer, 2269-2, were synthesized at the Biotechnology Core Facility of Texas Tech University (Table 2.2). Plasmids containing the desired mutations were identified by sequencing using a model 310 Genetic Analyzer (Perkin-Elmer Applied Biosystems). The Y81 mutant series was prepared as described in Nes et al. (1999) using the Gene Editor system (Stratagene). Other mutagenesis was carried out using the QuickChange™ (Stratagene) Site-Directed Mutagenesis protocol, a PCR based procedure that utilizes a super-coiled, double-stranded DNA (dsDNA) vector with a gene insert and 2 synthetic oligonucleotide primers containing the desired mutation. The mutagenic primers, each complementary to opposite strands of the vector, are extended during temperature cycling by *Pfu* DNA Polymerase. Upon incorporation of the mutated sequence into full-length dsDNA, a mutated plasmid containing staggered nicks is generated. Following PCR amplification, the product is treated with *DpnI* to degrade the unmethylated parental template DNA. The nicked vector is then transformed into competent cells and cultured. The plasmid DNA is isolated and prepared for sequencing. Once the correct sequence is confirmed, then the plasmid can be transformed into BL21(DE3) cells and grown as previously described.

Photolabeling of the SMT with AdoMet

AdoMet has been shown to specifically label the methyltransferases, using high intensity short wave UV radiation (Subbaramaiah and Simms, 1992). *S*-Adenosyl-L-[methyl-³H]methionine (20-50 μCi) is incubated with purified enzyme (2-10 μg) in resuspension buffer, pH 7.5 in a final volume of 100 μl. Incubations are carried out in

round bottom 96-well microtiter plates at 4°C. Labeling of [³H]AdoMet is induced by irradiating the samples with short wave UV light at 254 nm from a Multi-Ray UV lamp with a 1.0-cm distance between the light source and the sample. After irradiation, 1 volume of 2 x sample buffer is added to the labeling mixture, boiled for 10 minutes, and subjected to 12% SDS-PAGE as per Laemmli (1970). The gel is stained with Coomassie Blue, and the labeled proteins can be analyzed by fluorography.

The labeling mixture is also separately subjected to proteolytic digestion by trypsin as described previously. Tryptic peptides are separated on a C₁₈ reverse phase HPLC column with a flow rate of 1 ml/min: 0-85% acetonitrile with 0.25% trifluoroacetic acid, pH 6.0 for 80 minutes. HPLC was performed with a µBondapak C₁₈ reverse phase column. The radioactivity of the individual fractions was determined by liquid scintillation counting.

Western Blotting

Antibodies raised against the HIC pure SMT (yeast-recombinant) were provided by Monsanto. The yeast-recombinant SMT was generated in 1997 in the Nes Laboratory and sent to Monsanto. The anti-serum was purified as described in the following section. The protocol for immuno-blotting follows that described in Copeland's Methods for Protein Analysis (1994). The pure SMT is run on SDS-PAGE as described by Laemmli (1970). The gel is not stained with Coomassie Blue but instead is soaked in Towbin's transfer buffer (20 mM Tris-HCl, 150 mM glycine, pH 8.0, 20% methanol, v/v) for 30 minutes. A nitrocellulose membrane and 4 sheets of Whatman filter paper, cut to match

the dimensions of the gel, are soaked in Towbin's transfer buffer for at least 5 minutes. Then the gel, membrane and filter paper are assembled in the transfer sandwich and loaded into the electrophoretic tank filled with Towbin's buffer. The protein is transferred to the membrane by electrophoresis at 100 V (constant voltage) for 1 hour. The membrane now is fixed with the protein and can be prepared for antibody blotting.

The goat/anti-rabbit Alkaline Phosphatase Immunoblot Kit is purchased from BioRad. The membrane is immersed in blocking solution (3% gelatin in Tris buffered saline, TBS, 20 mM Tris-HCl, pH 7.5, 500 mM NaCl) and agitated for 1 hour at room temperature. The blocking solution is decanted and washed with TTBS (0.05% Tween-20 in TBS) for 5 minutes. The first antibody solution (1% gelatin in TTBS with 200 μ l purified SMT antibody) is then added to the membrane and gently agitated overnight at 4°C. The first antibody solution is decanted and the membrane washed with TTBS for 5 minutes. The second antibody (33 μ l of goat/anti-rabbit serum in 1% gelatin in TTBS) is added to the membrane and gently agitated for 2 hours at room temperature. The second antibody solution is removed by washing 3 times with TTBS. Lastly the membrane is immersed in color development reagent (filtered Alkaline Phosphatase solution with 1% v/v color reagents A and B, added just prior to use) with gentle agitation at room temperature. Lower concentrations of detectable protein amounts should be visible in 30 minutes. The development is stopped by removing the color reagents and adding ddH₂O. At this point, the blot can be scanned or photographed to record the positive immuno-reaction.

Purification of the Antibody

The Serum IgG Purification Kit was purchased from BioRad and the protocol for purification follows that described in the kit. All buffers and columns described are contained in the kit and are prepared either by reconstitution or dilution. Discard the buffer above the top frit of an Econo-Pac serum IgG column and snap off the bottom tip. Prewash the column for first time use only. Wash the column with 40 ml of regeneration buffer (rabbit). Allow the buffer to drain to the top of the frit. Equilibrate the column with 30 ml of application buffer. Apply the prepared sample to the column (the sample is prepared by pre-equilibration with rabbit application buffer). Elute the IgG with 20 ml of application buffer. For a more precise collection method, collect fractions of volumes approximately equivalent to that of the sample applied. Determine the absorbance at 280 nm of each fraction using a spectrophotometer and combine effluent tubes containing the unbound protein peak. Wash the column with 30 ml of application buffer to regenerate the column or store at 4°C in application buffer containing 0.02% sodium azide.

Equilibrium Dialysis Experiments and Determination of Binding Constants

Binding constants as a function of sterol suitability without catalysis were investigated using equilibrium dialysis methods as outlined by Copeland in Methods of Enzymology (2000). Using radioactive sterols (Le and Nes, 1986), the concentration of free and enzyme-bound ligand was determined by conversion of radioactive counts via

scintillation counting to mass of enzyme, ligand and enzyme-ligand complex. Binding constants are calculated in the following manner:

$$K_d = (\text{free enzyme})(\text{free ligand})/\text{enzyme-ligand complex}$$

$$\Delta G_{\text{binding}} = RT \ln K_d$$

$$\Delta\Delta G = RT \ln (K_{d,\text{mut}}/K_{d,\text{native}}).$$

The Langmuir Binding Isotherm utilized for visual confirmation of binding constants is a plot of % bound ligand, semi-log, vs. concentration of ligand, usually in the μM range.

Each equilibrium dialysis experiment is performed using the same ratios and concentrations of enzyme and substrate as described in the assay protocol section, except that the individual tubes are up-scaled 10 times. For example, the total volume is 6 ml instead of 0.6 ml. This is done in order to ensure that the volume is sufficient to cover the dialysis tubing containing the protein solution. Two different types of experiments were performed, concentration dependence (0 to 100 μM) of ligand binding and time-course dependence (0-24 hours) of binding. All radioactive counts are normalized to the preferred substrate for yeast SMT, zymosterol. A control experiment in which the enzyme was not added to the dialysis tubing was performed in order to determine the amount of background radioactivity. Before calculation of K_d , this background limit would be subtracted from the total radioactive counts. The specific activities of the substrates are as follows: zymosterol, 3×10^8 dpm/mg; AdoMet, 2×10^8 dpm/mg; ATP, 2.1×10^9 cpm/mg; 24-epiminolanosterol, 2.5×10^7 dpm/mg; and lanosterol 7.5×10^8 dpm/mg.

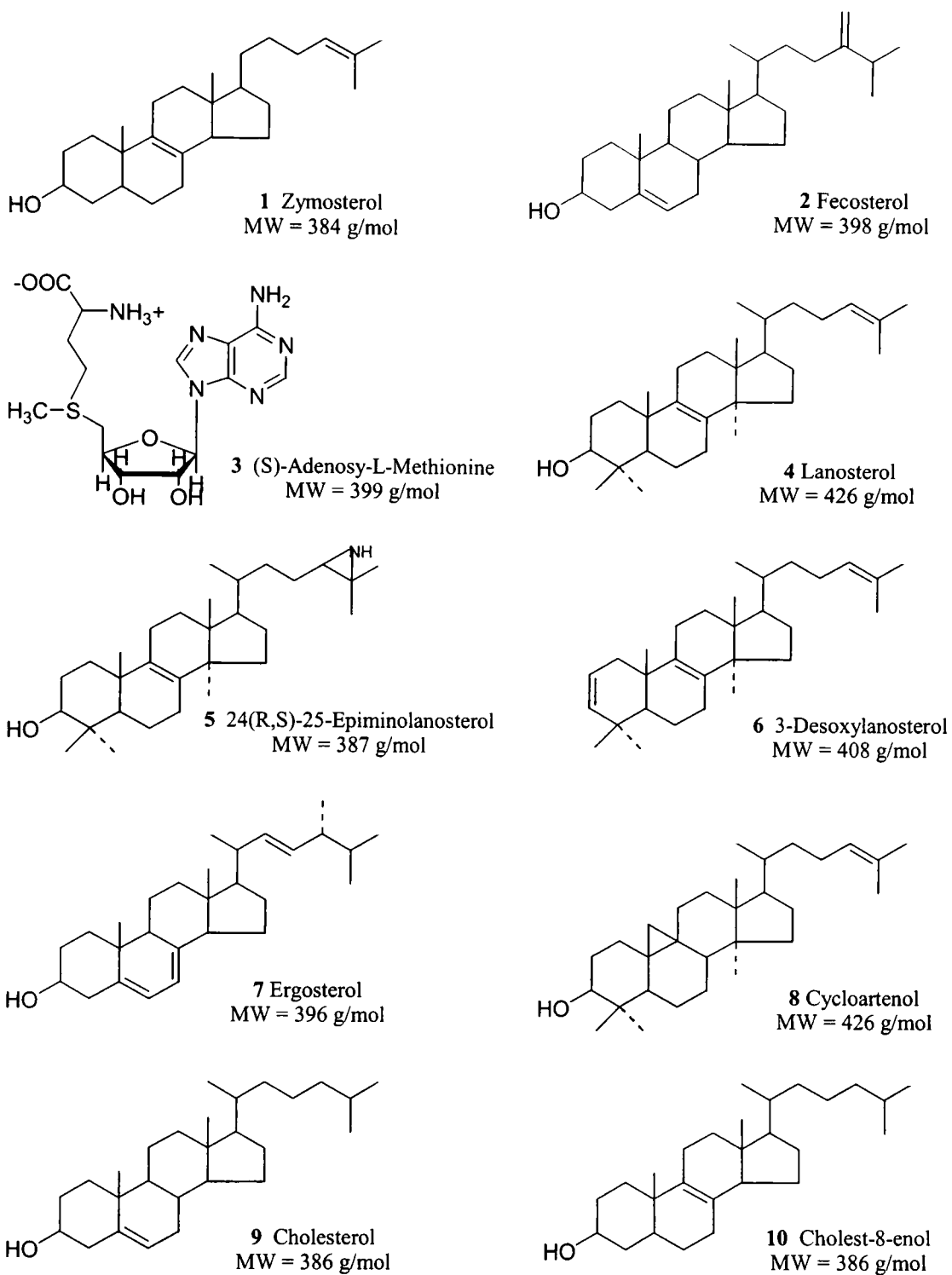


Figure 2.1. Substrates and Inhibitors of the yeast SMT enzyme. The trivial name is given with the molecular weight of the compounds stated below each name, respectively.

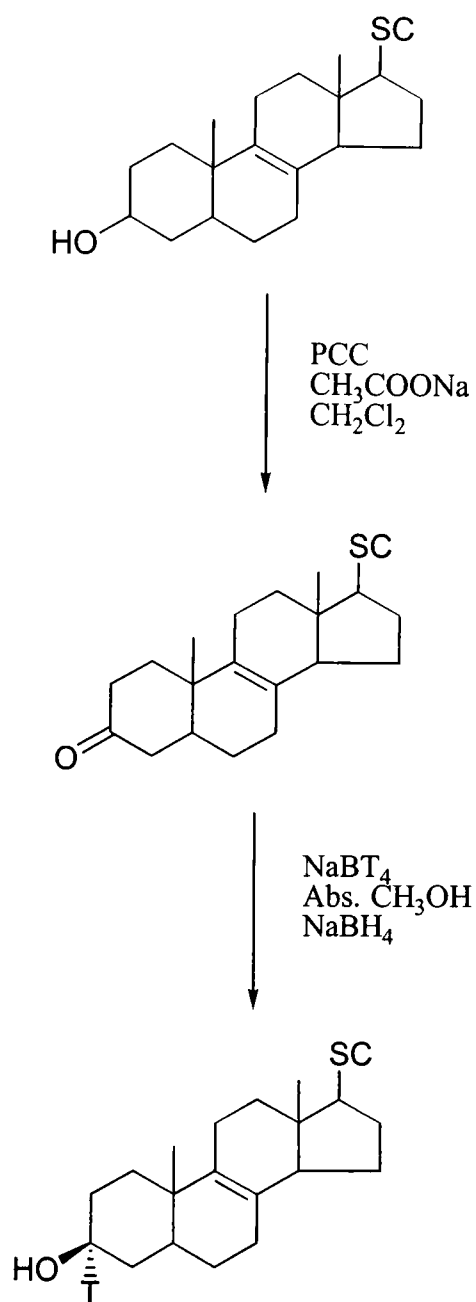


Figure 2.2. Preparation of the 3-tritio Δ^8 sterols (SC-sterol side chain).

Table 2.1: Quantification of the yeast SMT.

Sample #	W (mg)	Error (%)	B (mg)	Error (%)	U (mg)	Error (%)	S (mg)	Error (%)
1	2.9	0	0.54	82	3.5	19	2.5	18
2	2.8	0	0.50	82	3.5	24	2.5	12

Note: The mass by gravimetric determination is assumed correct in calculating percent error. Samples 1 and 2 were obtained from 2 different Mono Q preparations of the pure enzyme.

W- mass by gravimetric determination

B- mass by the Bradford method

U- mass by ultraviolet scan

S- mass by SDS-PAGE determination

Table 2.2: Oligonucleotide primers synthesized for mutagenesis and sequencing.

Primer Name	Oligonucleotide Sequence ¹
Y81F	ACA GAT TTC TTT GAA TAT GGT TGG
Y81W	ACA GAT TTC TGG GAA TAT GGT TGG
Y81A	TAT AAC GTC GTT ACA GAT TTC GCT GAA TAT GGT TGG GGT TCC TCT
Y81L	ACA GAT TTC CTT GAA TAT CGT TGG
T78V	TAC TAT AAC GTC GTT GTA GAT TTC TAT GAA TAT
P133L	GTT GGG GGC CTA GCA ACA GAG
2269-2	CGA TTA CCA AAT TGC CAG

Note: ¹ The mutagenic bases are highlighted.

CHAPTER III
ALLOSTERIC MODULATION OF THE STEROL
METHYL TRANSFERASE ENZYME

Allosteric Modulation by ATP

SMT enzymes are found in all groups of microorganisms. The SMT from *S. cerevisiae* catalyzes the bisubstrate, sterol dependent C-methyl group transfer reaction from AdoMet that results in the incorporation of an exocyclic 24(28)-methylene group in the sterol side chain. Normally this involves the conversion of zymosterol to fecosterol. At least 14 SMT enzymes have been cloned and sequenced from plants and fungi as revealed in the GenBank. The amino acid sequences of these proteins are highly conserved, suggesting functionally equivalent binding sites that may be placed in different three-dimensional structures. Based on studies by Nes et al. (1998) and Niewmierzycka and Clarke (1999) there appear to be 10 motifs of sequence homologies in AdoMet binding proteins as verified by crystal structures of 9 such proteins. Motifs I, II, III and post-I have been shown to directly interact with AdoMet but the identity of the other motifs has not been completely defined. However, nucleotide and nucleic acid binding sequences are known to exist in the methyltransferase family of enzymes (Kagan and Clarke, 1994, Figure 3.1). Knowing the significance of ATP (structure shown in Figure 3.2) as signaling molecule in metabolic pathways such as glycolysis, ATP and other signaling compounds were tested as effectors for the SMT in the sterol biosynthetic pathway.

Kinetic Studies with the Native Recombinant SMT

The SMT enzyme was assayed in the presence of ATP with 50 μg of SMT and 50 μM zymosterol. The activity of the enzyme was affected by the addition of ATP to the reaction mixture (Figure 3.3). At 400 μM ATP, the activity of the enzyme was increased three-fold from a specific activity of 200 to 600 pmol/min/mg protein. Similar assays were performed with ADP, AMP, and in phosphate containing buffer but there was no change in the activity of the enzyme. The enzyme was assayed in the presence of ATP, zymosterol, and ergosterol (sterol insert in yeast which acts as a feedback-inhibitor of the enzyme's activity). Ergosterol concentration was varied from 0 to 200 μM . The IC_{50} for ergosterol (previously reported to be 65 μM) was increased to 100 μM (Figure 3.4).

To demonstrate specific binding of the enzyme by ATP, equilibrium dialysis experiments were performed to determine K_d . Without the presence of zymosterol and AdoMet (no catalysis), ATP was bound by the enzyme in the concentration range similar to the preferred substrates as shown by the binding isotherm (Figure 3.5). Due to the discovery that ATP affects activity of the native SMT, equilibrium dialysis experiments were performed with and without ATP for a variety of sterol substrates to determine if ATP increased binding of the sterol to the enzyme. The results are summarized in Table 3.1. ATP appears to have no effect on the equilibrium binding of the sterol to enzyme.

After it was established that ATP had some effect on activity, the kinetic parameters were measured with varying zymosterol concentration and ATP and AdoMet held at a constant concentration. The results of the Lineweaver-Burke plots are shown in

Figure 3.6. Graphical analysis of the data with and without ATP was used to calculate K_m and V_{max} for the enzyme. Without ATP, the K_m for zymosterol was determined to be 13 μM . With ATP the K_m remained fairly constant at 20 μM . However, the addition of ATP altered V_{max} from 728 to 1311 specific activity units. The results are summarized in Table 3.1.

Kinetic Studies with the Y81F Mutant SMT

Y81F, a mutant SMT, was also assayed in the presence of ATP. As previously reported (Nes et al., 1999), this mutant will perform a second *C*-methyl transfer to generate 3 doubly alkylated products at C24. Fecosterol, the C_1 -methylated product of the normal enzymatic reaction, is a substrate for the second *C*-methyl transfer reaction. When the Y81F mutant enzyme was assayed in the presence of zymosterol and increasing ATP, it behaved similarly to the native SMT. However, when the mutant enzyme was assayed in the presence of fecosterol and ATP, as ATP increased the activity was inhibited (Figure 3.7). When the Y81F enzyme was functionally complemented into *erg6* cells (yeast strain deficient for the SMT), the second alkylation was not apparent even though *in vitro* studies show a high degree of conversion (unpublished data). The cells are grown under anaerobic conditions and ATP is present in similar concentration within the cell as described in the previous experiments (Rose, 1969). The results are interpreted to imply that ATP may help guide which products are made and the degree of alkylation at C24 under normal physiological conditions.

Kinetic Studies with *Arabidopsis thaliana*

A native construct of the *A. thaliana* SMT cDNA was successfully subcloned into *E. coli* (Zhou, 1998). The enzyme was partially purified and the function studied in vitro. Since the enzyme preparation generated from this bacteria will necessarily contain a single SMT species, it was possible to determine unambiguously whether the C₁- and C₂-activities are generated from a single enzyme by analyzing the enzyme-generated products. Sterol specificity studies established that the enzyme recognized both cycloartenol (C₁-methyl transfer) as well as 24(28)-methylene lophenol (C₂-methyl transfer) as substrates. The second alkylation is preferred by the SMT II isoform of the *A. thaliana*.

The SMT II from *A. thaliana* was assayed in the presence of ATP. When 400 μM ATP was added to the enzyme preparation, the substrate acceptability was modulated with a three-fold increase of activity for cycloartenol whereas a compensating four-fold decrease in substrate acceptability for 24(28)-methylene lophenol was detected. Sitosterol but neither ergosterol nor cholesterol was found to down-regulate the activity of the *A. thaliana* SMT. Experiments by the West group (1979) indicate that the rate of terpenoid synthesis in plants may be under energy charge regulation involving ATP, which suggests that phytosterol synthesis can be under a similar control system. The ability for sitosterol to down-regulate SMT activity and ATP to activate SMT activity provides the biochemical basis for SMT to act as a branch-point enzyme regulating the synthesis of sitosterol production.

ATP Binding Site	(1)	VGLVAGGKSK
Saccharomyces cerevisiae	(346)	VGLVAGGKSK
Schizosaccharomyces pombe	(352)	KGLIEGGETH
Candida albicans	(349)	VNLVEGGRQK
Neurospora crassa	(355)	DGLVAGAKKK
Triticum aestivum	(338)	EGLVEGGKKE
Glycine max	(340)	EGLVEGGKRE
Ricinus communis	(319)	EGLVEGGRKE
Zea mays	(319)	EGLVEGGKKE
Arabidopsis thaliana	(313)	EGLVDGGRRE
Arabidopsis thaliana 2-1	(332)	DYLTRGGETG
Oryza sativa (24-methyl lophenol)	(337)	QHLTRGGETG
Oryza sativa subsp. japonica (cycloartenol)	(324)	EGLVEGGKKE
Arabidopsis thaliana 2-2	(332)	DYLTRGGETG
Nicotiana tabacum 1-1	(322)	QGLVGGAKKG
Nicotiana tabacum 1-2	(319)	EGLVGGAKKG
Nicotiana tabocum 2-1	(333)	DYLSKGGEKG
Nicotiana tabacum 2-2	(327)	DYLAKGGDKG
Pneumocystis carinii	(335)	DSLVKAGKKE

Figure 3.1. Amino acid composition of the proposed ATP binding site aligned against the sequences of related SMTs.

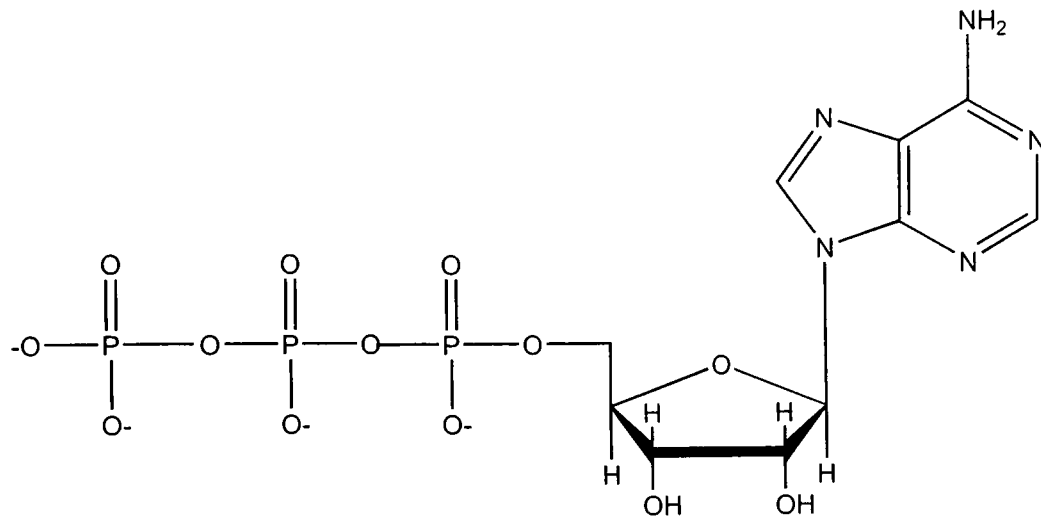


Figure 3.2. The structure of Adenosine Triphosphate.

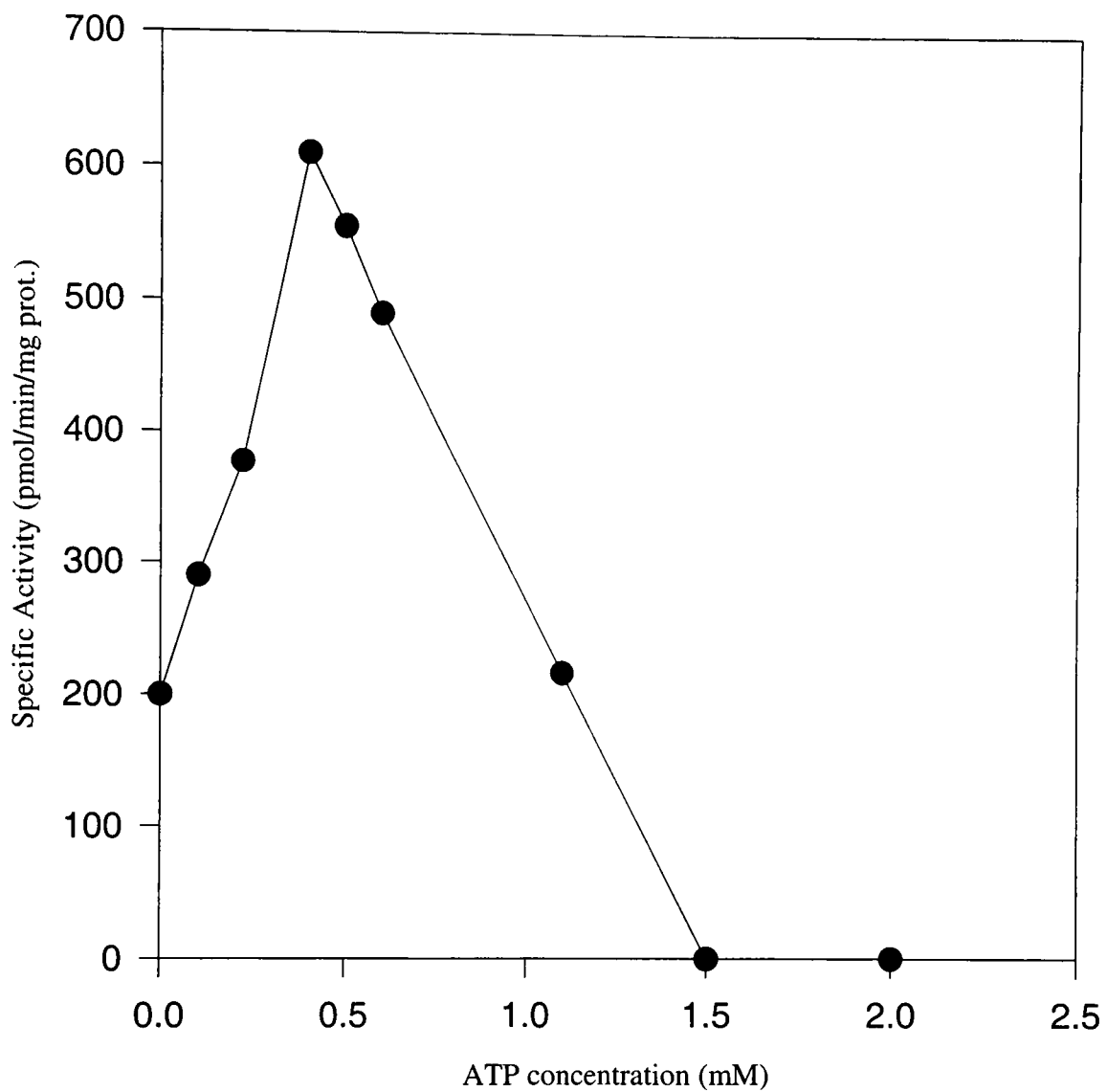


Figure 3.3. Variations in the activity of the native SMT with 50 μ M zymosterol and increasing ATP concentration.

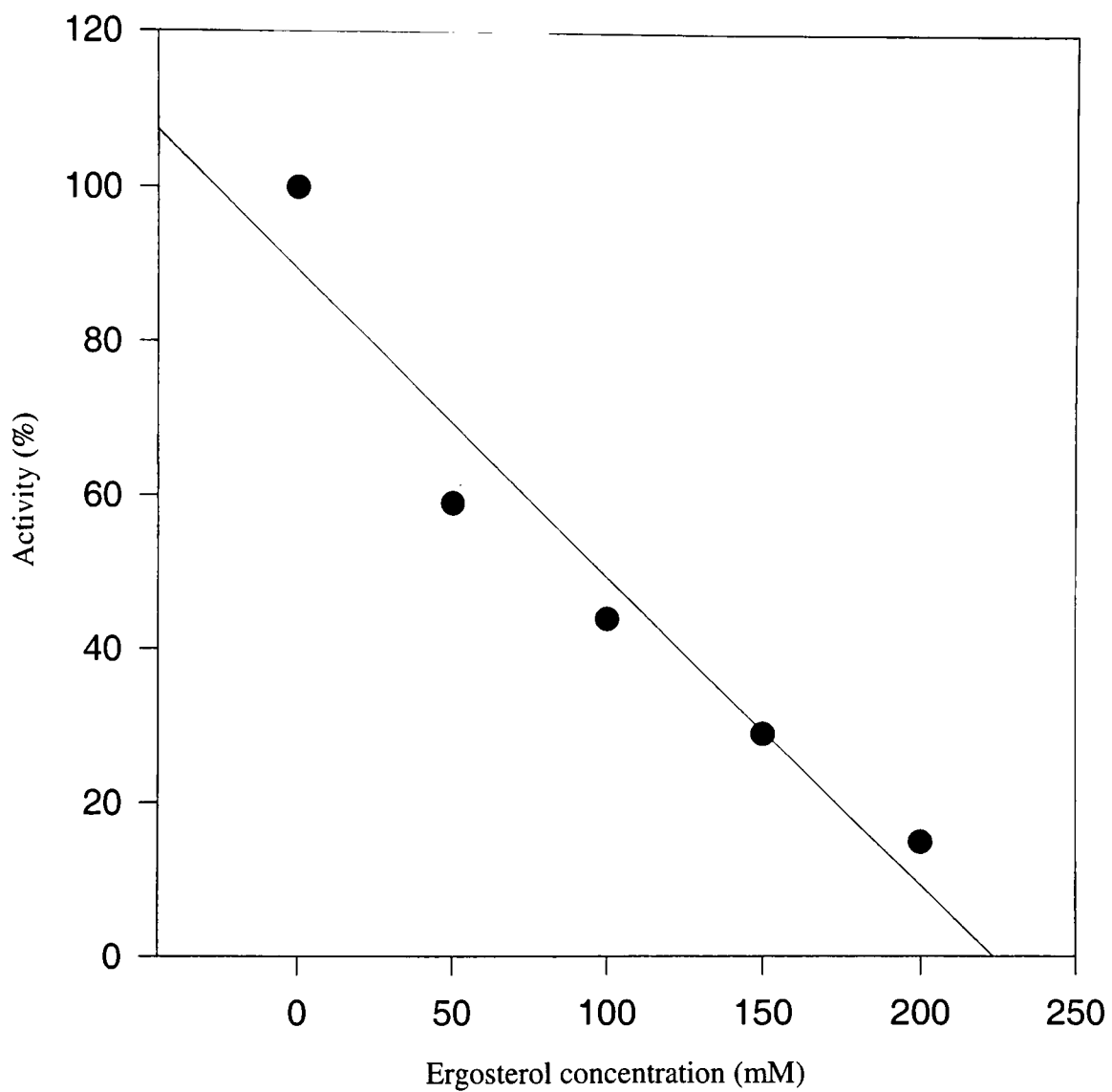


Figure 3.4. Inhibition plot for the native SMT with 50 μ M zymosterol and increasing ergosterol in the presence of 0.4 mM ATP.

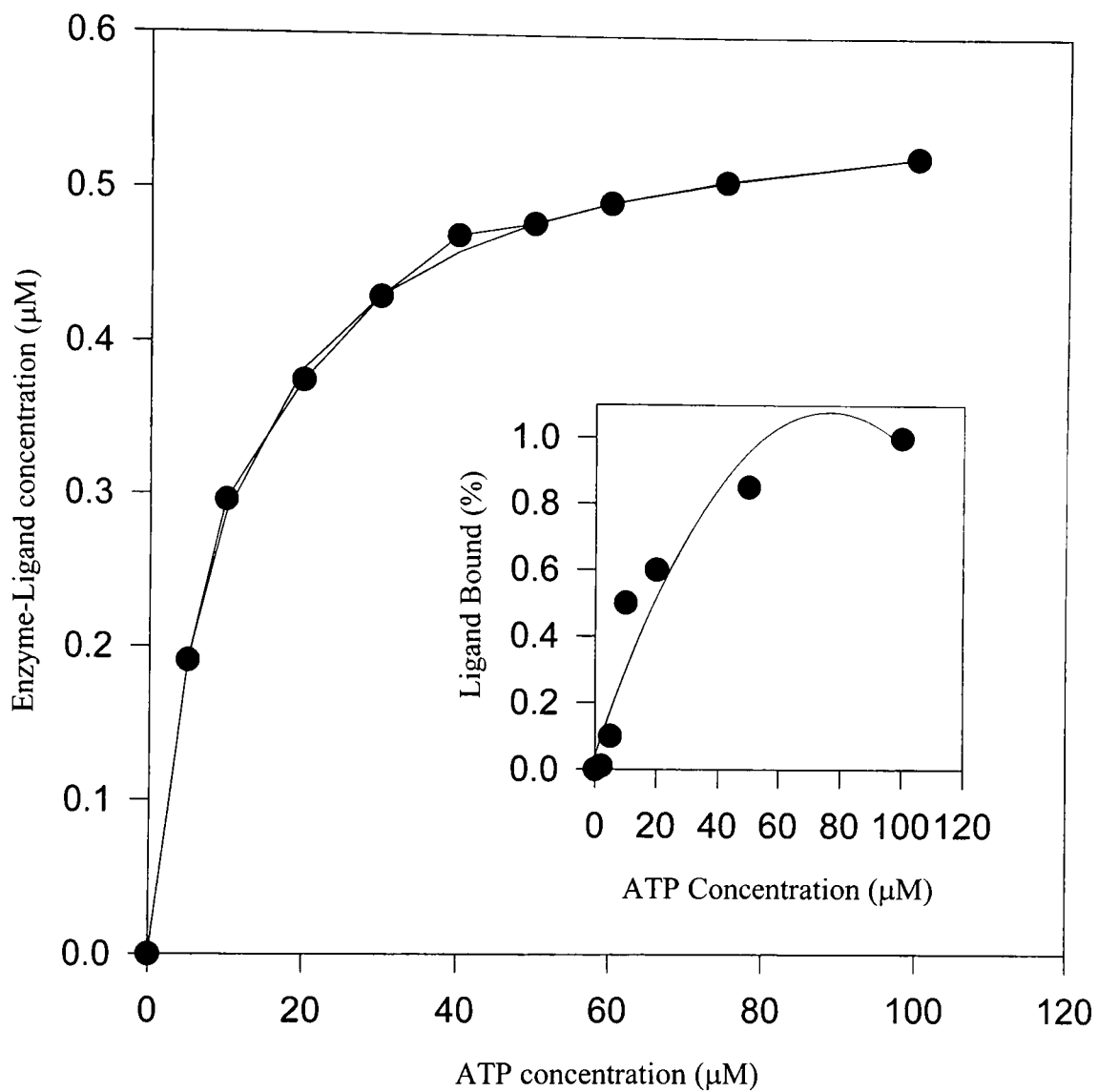


Figure 3.5. Binding isotherm for the native SMT in the presence of the increasing ATP concentration. K_d is determined from inset plot at 50% ligand bound to the enzyme. Percentage bound is calculated from radioactive counts.

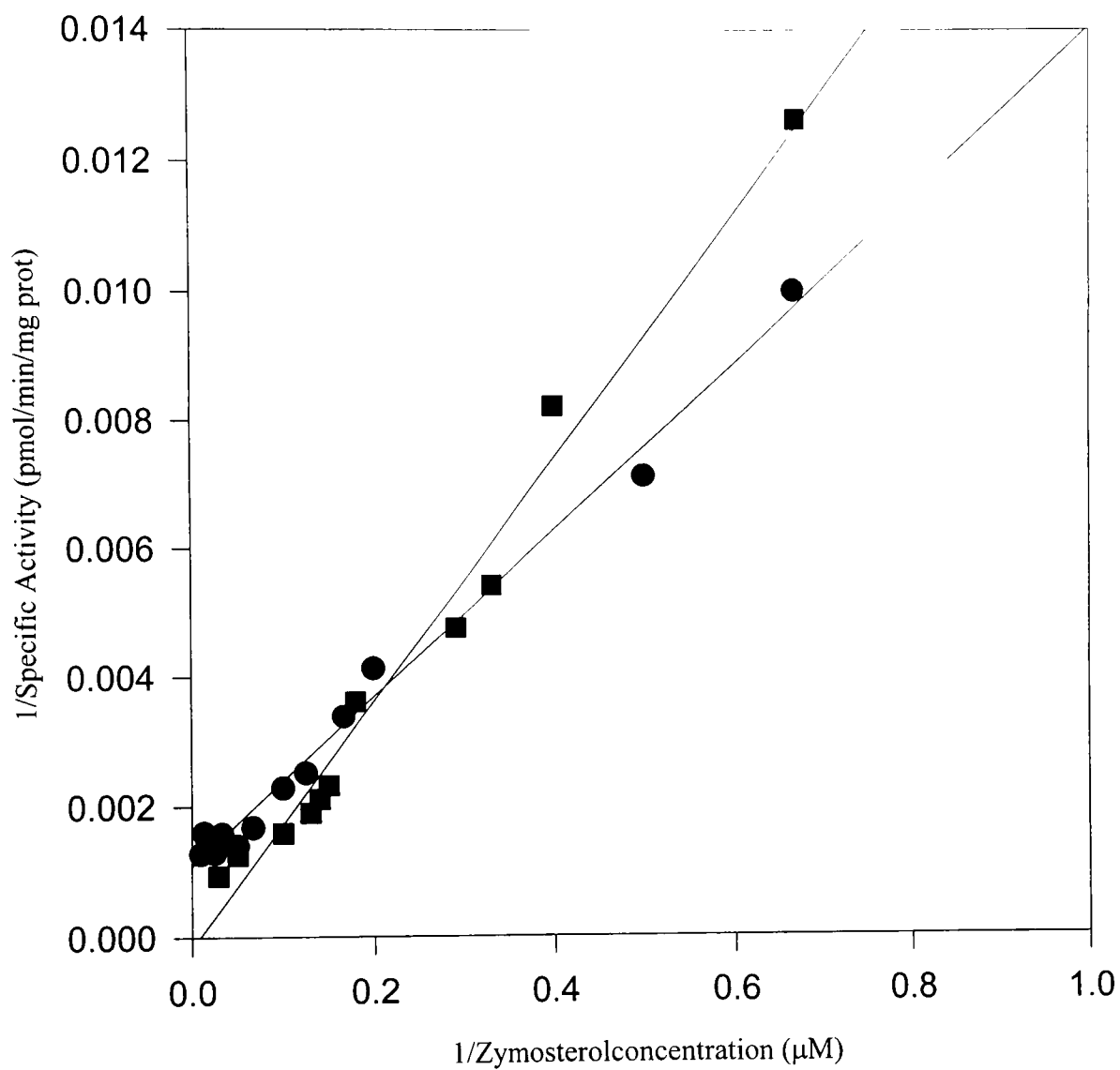


Figure 3.6. Lineweaver-Burk plot of the native SMT with ■ and without ● 0.4 mM ATP.

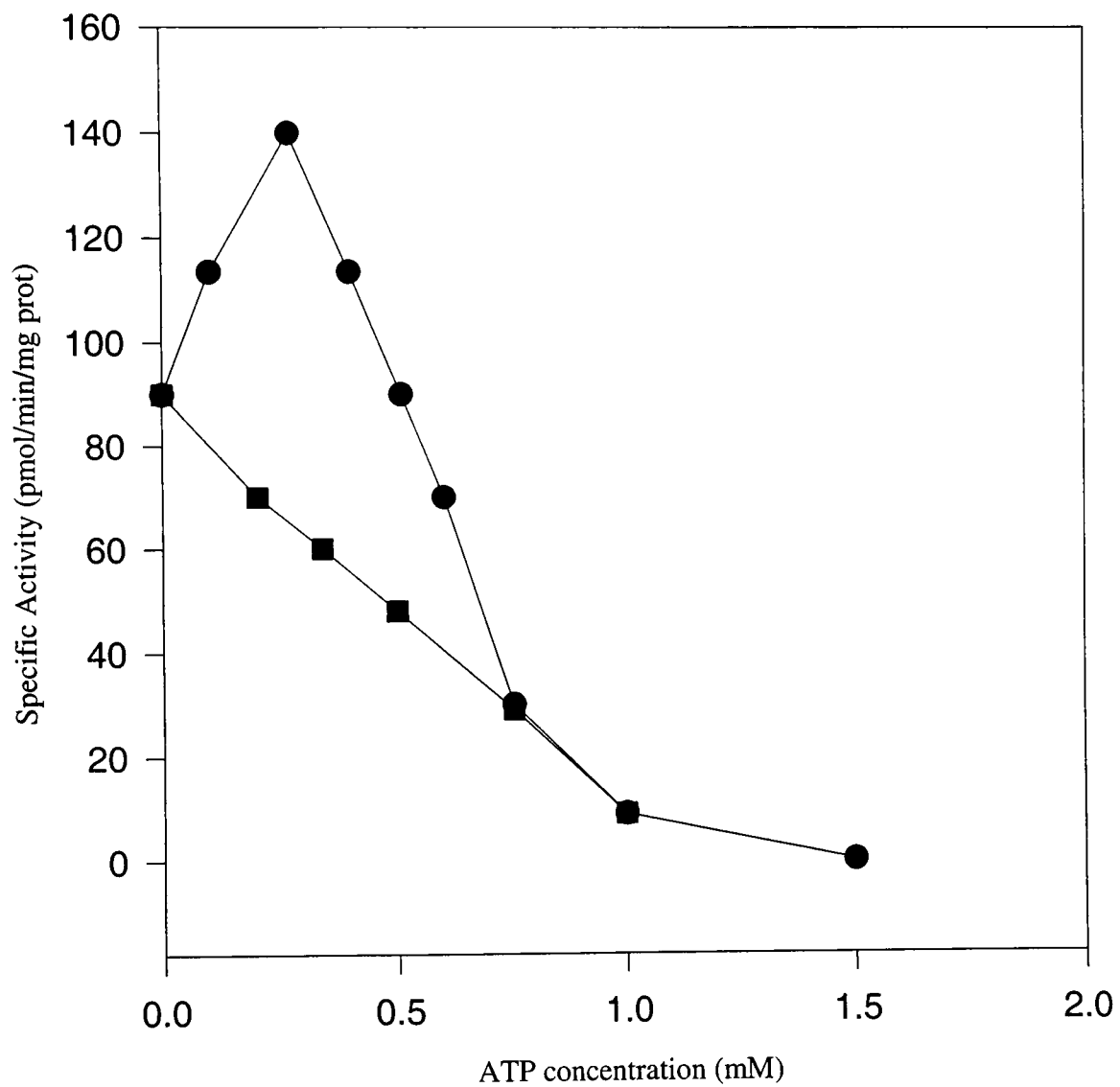


Figure 3.7. Variations in the activity of the mutant Y81F SMT with 50 μM fecosterol, 50 μM zymosterol • , and increasing ATP concentration.

Table 3.1: Kinetic parameters for the substrates of the yeast SMT (NP- non-productive, NA- non-applicable).

Substrates	K_m (μM)	k_{cat} (s^{-1})	K_d (μM)	K_i (μM)
Zymosterol	12	10.9×10^{-3}	4.3	NA
Fecosterol	38	2.67×10^{-3}	3.5	NA
3-Desoxy-lanosterol	NP	NP	76.2	NA
Lanosterol	NP	NP	22.0	NA
Ergosterol	NP	NP	7.5	65
Cycloartenol	NP	NP	25.5	NA
Cholesta-8-enol	NP	NP	26.0	NA
Cholesterol	NP	NP	16.0	NA
24-Epimino-lanosterol	NA	NA	8.5	0.01
AdoMet	12	10.9×10^{-3}	4.6	NA

CHAPTER IV
KINETIC AND THERMODYNAMIC CONTROL
OF SUBSTRATE-ENZYME INTERACTIONS

SMT Substrate Specificity

A major determinant which controls molecular diversity in product structure, stereochemistry and of enzyme efficiency is believed to be the precise three-dimensional fit between the sterol substrate-AdoMet-enzyme in the active center of the SMT. Although the reaction pathways involved in sterol *C*-methylation have been studied, little is known about the active site topography of any SMT or the manner in which a SMT enzyme imposes a particular conformation on its amphiphilic substrate, precisely controls the resulting methylation-elimination reaction and establishes the binding order and release of $\Delta^{24(25)}$ - and $\Delta^{24(28)}$ - substrate. The lack of availability of pure enzyme (Table 4.1) and of common substrates to test the enzyme activity has delayed progress in characterizing SMT's. These issues stimulated the Nes group to isolate from nature or synthesize over 100 substrate analogs to determine the substrate specificity of SMT from fungi and plants. Zymosterol (Figure 2.1), a $\Delta^{8,24}$ -sterol, was isolated from bakers yeast or prepared synthetically. With this and other compounds available, the yeast SMT was tested with different sterol substrates that differed in a single structural feature, but otherwise were similar to the natural substrate, zymosterol. By examining the magnitude of the K_m values and the ratio of V_{max}/K_m of sterols structurally related to the natural substrate, it has been possible to determine the relative structural requirements of sterols

necessary for recognition and to measure the substrate acceptability for catalysis. Steady-state kinetic measurements were performed using the standard enzymatic assay as described in Chapter II and the results summarized in Table 3.1.

Four domains of the sterol acceptor molecule were evaluated for their relevance to substrate acceptability (Figure 1.5). The principal determinants for binding were shown to be the nucleophilic features at C-3 and C-24 of the sterol, represented by domains 1 and 4. Based on the catalytic competence of a series of substrate analogs in which the side chain structure and stereochemistry were modified stereochemically and otherwise, and on the assumption of restricted side chain motion during the course of the enzymatic C-methylation, a direct one-to-one relationship was found to exist between the absolute configuration at C-20 and the orientation of the side chain to the right of C-20, represented by domain 3. In addition, structure-activity tests with several nuclear variants indicated the structure of the nucleus should be flat at initial binding. Minor changes in the structure of the nucleus by locating the double bond in different rings which can control the β -orientation of the side chain at C-17 was shown to significantly affect activity. Thus subtle changes in the tilt of the 17(20)-bond with the influence of a 1,3-diaxial relation of the C-18 methyl group to C-20 hydrogen atom clearly serve to hinder rotation of the side chain into a staggered or pseudocyclic conformation, represented by domain 2. The β -orientation of the side chain at C-17 and the right-handed conformation at C-20 also facilitates the control of configuration at C-24 in sterol C-methylation transfer reactions, since the C-methyl bridged carbenium ion intermediate is generated in a consistent geometry for H-24 to C-25 hydride migration to proceed on the *Re*-face of

the substrate double bond and since C-24-C-25 bond rotation is restricted. The sterol specificities of SMT confirm that zymosterol is the preferred substrate for the yeast SMT and that neither lanosterol nor cycloartenol will bind productively for catalysis.

Despite the fact that lanosterol does not bind to the SMT productively, 24-epiminolanosterol that differs from lanosterol only at position 24 in the sterol, is a potent inhibitor of the SMT (Venkatramesh et al., 1996) with a K_i of 10 nM well below K_m values for the SMT. How is it then possible for 2 such similar sterols to behave so differently? Additionally, it has been much debated whether or not 24-epiminolanosterol is positively charged at physiological pH and therefore competes with AdoMet binding because AdoMet is charged at physiological pH. In 1999, Boissy et al. published the three-dimensional structure of a sterol carrier protein that had been co-crystallized with ergosterol. The sterol-binding pocket was shown to be a flexible loop that is lined with aromatic and hydrophobic residues. This hydrophobic tunnel did not have a defined structure such as a helical or pleated form but rather was induced to form a hydrophobic pocket around the sterol upon binding. Based upon these results, it is hypothesized that sterols with comparable features will bind with similar efficacy to the enzyme. Equilibrium dialysis, a method for studying binding without catalysis was investigated.

Protein-Ligand Binding Equilibria

Enzymes catalyze the transformation of substrate to product. For this reaction to proceed, however, the enzyme and substrate must first encounter each other and form a binary complex in a specific site on the enzyme (Copeland, 2000). The substrate in this

context is referred to as the ligand (L) and the enzyme the receptor (R). Mathematical expressions can be derived to determine the equilibrium constant of dissociation and graphical expressions for studying the more complex protein-ligand interactions. The assumption is made that the receptor has at least one binding site for the ligand and so any receptor is either free or ligand bound. Likewise, any ligand molecule can either be free or receptor bound. This assumption leads to the following equations:

$$[R] = [RL] + [R]_f$$

$$[L] = [RL] + [L]_f$$

$$K_d = ([R]_f - [RL]) [L] / [RL]$$

$$[RL] = [R]_f [L] / K_d + [L]$$

An equilibrium will be established between the free and bound forms of the receptor. The equilibrium dissociation constant is calculated by the equation given in experimental methods. The strength of binding or binding affinities of the ligand-receptor complexes are inversely proportional to their K_d values; the tighter the ligand binds, the lower the value of the dissociation constant. Thus, dissociation constants can be used to compare affinities of different ligands for the same receptor. The dissociation constant can be related to the Gibbs free energy of binding, the thermodynamic parameter for this process by the equation described in the experimental methods section. It is very common for affinity to be expressed as a dissociation constant because the constant will have units of molarity and thus can be equated with a specific ligand concentration (Copeland, 2000).

Equilibrium Studies on the Native Substrates

It was necessary to first set-up all experimental parameters with zymosterol, the preferred substrate for the yeast SMT. As discussed in experimental methods, the amount of enzyme, buffer and substrate were proportionately held constant to assay conditions that have been proven over time. Conveniently, the Nes collection of sterols contains a wide variety of radiolabeled substrates in large quantity, however, it was necessary for the investigator to radiolabel several of the substrates used especially zymosterol. The radioactive uptake of zymosterol to SMT was measured as a function of time to determine when the receptor would be bound to saturation. Also, a control was performed in which radioactive uptake of zymosterol was counted without the presence of the enzyme. Samples of the enzyme were also taken periodically to confirm activity (assay) and integrity (SDS-PAGE). The first substrates to be tested were zymosterol, fecosterol, and AdoMet.

Radioactive uptake as a function of ligand concentration was measured for a definitive period of time and dissociation constants calculated. The results are summarized in Table 4.2. The enzyme bound all 3 substrates to 50% saturation at about 4 μM . This value is well within the same order of magnitude as the K_m values related to catalysis. The binding isotherms for zymosterol and AdoMet are shown in Figures 4.1 and 4.2, respectively. Enzyme concentration is calculated in the following manner:

$$\begin{aligned} [E] &= 50 \mu\text{g} = 5 \times 10^{-5} \text{ g} \\ 5 \times 10^{-5} \text{ g} / 173,200 \text{ g/mol} &= 2.87 \times 10^{-10} \text{ mol} \\ 2.87 \times 10^{-10} \text{ mol} / 0.0005 \text{ L} &= 0.574 \mu\text{M}. \end{aligned}$$

The binding isotherms give visual confirmation of calculated K_d values for the substrates (Copeland, 2000). Fecosterol, which is the product of the first C-methylation in yeast, binds with similar efficiency to zymosterol. The presence of the methylene at C-24 prevents proper orientation of the sterol in the active site for further methylation (Figure 4.3). This result disproves the idea that the so-called “harmful” features of the sterol prevent binding of sterols not normally catalyzed and that there must be separate active sites or even 2 enzymes responsible for the first and second alkylation in various SMTs. The mutation at tyrosine 81 in the yeast SMT further confirms this idea because the mutation allows for methylation of fecosterol (these results will be discussed more completely in Chapter VI).

Equilibrium Studies on Other Sterols

The lanosterol series; lanosterol, 24-epiminolanosterol, and 3-desoxylanosterol was studied. As described previously, lanosterol and 24-epiminolanosterol differ from each other at position 24 of the sterol. The binding isotherms for each are shown in Figures 4.4 and 4.5, respectively. The calculated values for K_d are shown in Table 4.2. As hypothesized, the binding affinity for each is relatively similar. Both sterols have dimethyls at C-4 that interferes with the hydrogen bonding potential of the hydroxyl at C-3 with the enzyme so that they are not bound with the same efficiency as zymosterol and subsequently are not methylated. 3-desoxylanosterol that does not contain the hydroxyl at C-3 binds to the SMT with relatively low affinity. 24-epiminolanosterol uptake by the SMT was measured in the presence of zymosterol and AdoMet separately, without

catalysis. Zymosterol was completely prevented from binding the SMT while AdoMet was bound with similar efficacy to the control binding study. In this study, the 24-epiminolanosterol was not radiolabeled and zymosterol and AdoMet were so that radioactive counts were a direct measure of uptake of the preferred substrates.

The binding efficiencies of 4 additional sterols were also studied and the resulting K_d values summarized in Table 4.2. Ergosterol, a $\Delta^{5,7,22}$ -sterol, the final sterol product and membrane insert for the yeast is bound by the enzyme with some efficacy allowing it to serve as a feedback inhibitor for the yeast (Venkatramesh et al., 1996). Cholesterol, cycloartenol, and Δ^8 -cholesterol (structures shown in Figure 4.3) bind to the SMT somewhat but not with enough efficiency to promote either catalysis or inhibition. Each of the 4 sterols lacks the double bond at C-24 that undoubtedly influences the positioning of the sterol for methylation.

Gibb's Free Energy of Binding

From the calculated equilibrium constant for each substrate, it is possible to calculate Gibb's free energy for binding, ΔG . For any spontaneous process at the given temperature, the sign of ΔG should be negative. One would expect that equilibrium binding between an enzyme and substrate should be spontaneous at temperatures close to biological norms. The change in free energy for zymosterol was calculated in the following manner:

$$\Delta G_{\text{binding}} = RT \ln K_d$$

$$R = 8.31 \text{ J/Kmol}$$

$$T = 32^{\circ}\text{C}, 305 \text{ K}$$

$$\Delta G = (8.31\text{J/K mol})(305\text{K}) \ln (4.3 \times 10^{-6}\text{mol})$$

$$= -31319 \text{ J}$$

$$= -31.3 \text{ kJ}$$

Gibb's free energy changes were calculated for each substrate that has been discussed in this chapter and the results summarized in Table 4.2

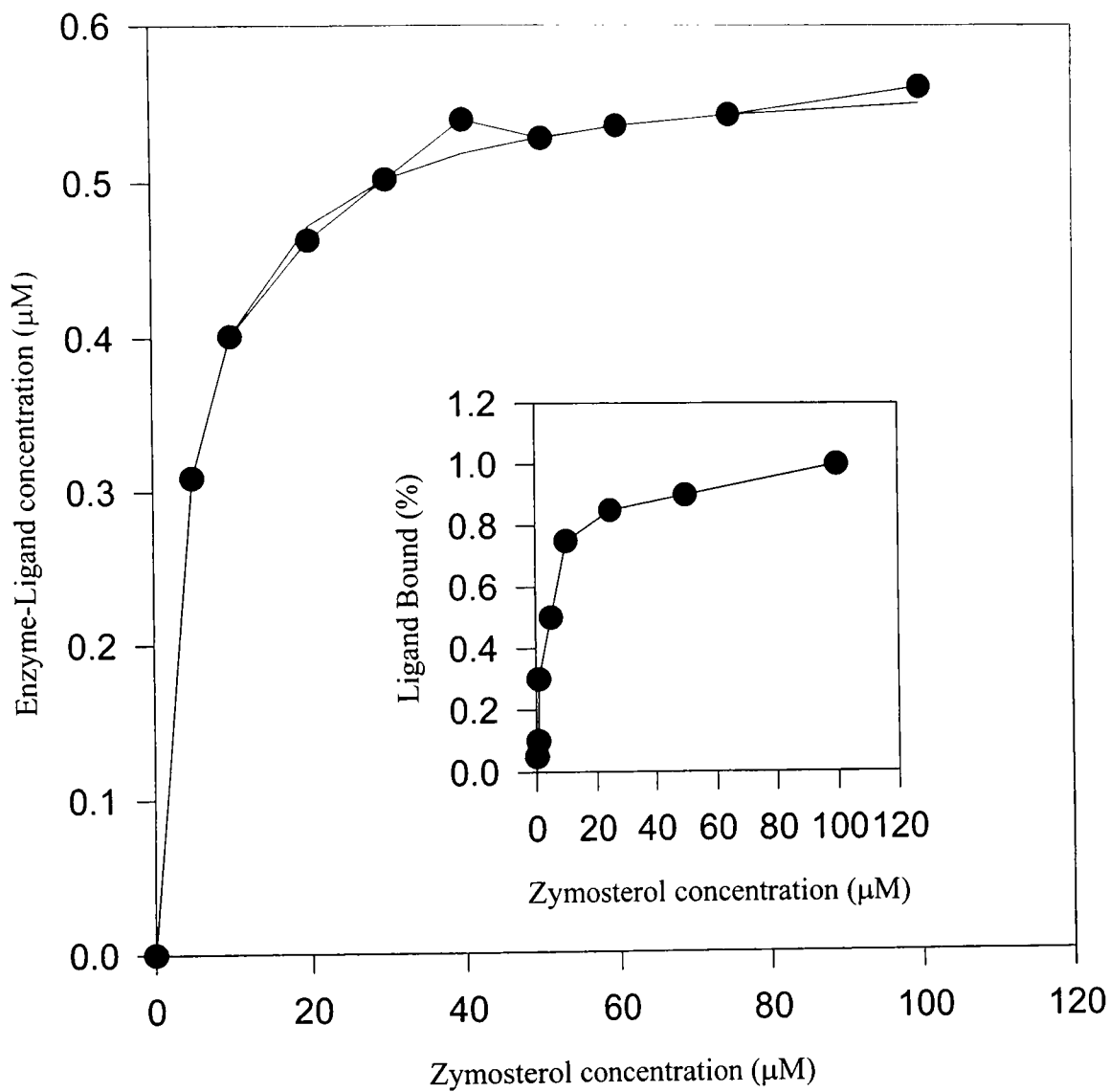


Figure 4.1. Binding isotherm for the native SMT in the presence of increasing zymosterol concentration. K_d is determined from inset plot at 50% ligand bound to the enzyme. Percentage bound is calculated from radioactive counts.

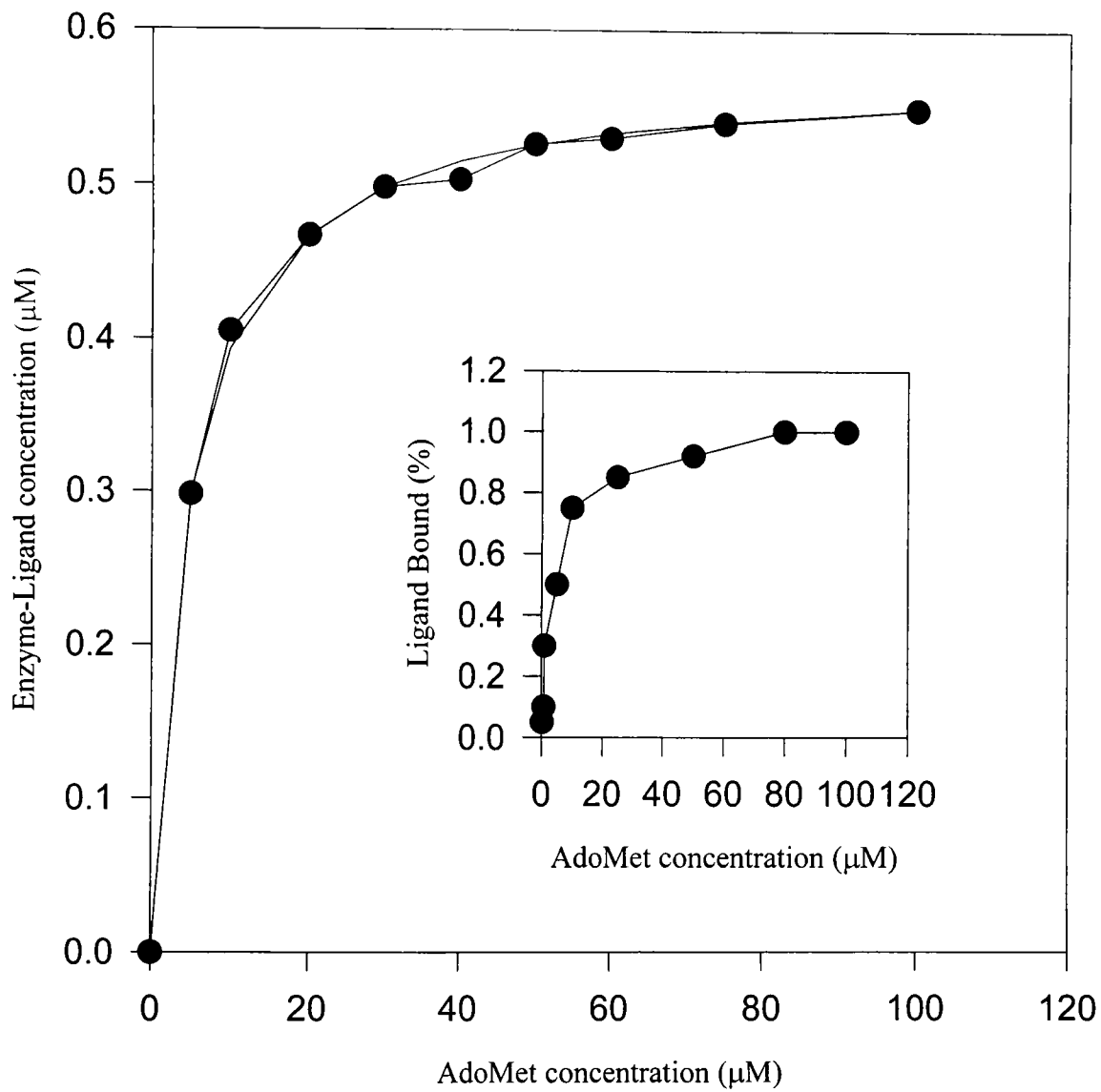


Figure 4.2. Binding isotherm for the native SMT in the presence of increasing AdoMet concentration. K_d is determined from inset plot at 50% ligand bound to the enzyme. Percentage bound is calculated from radioactive counts.

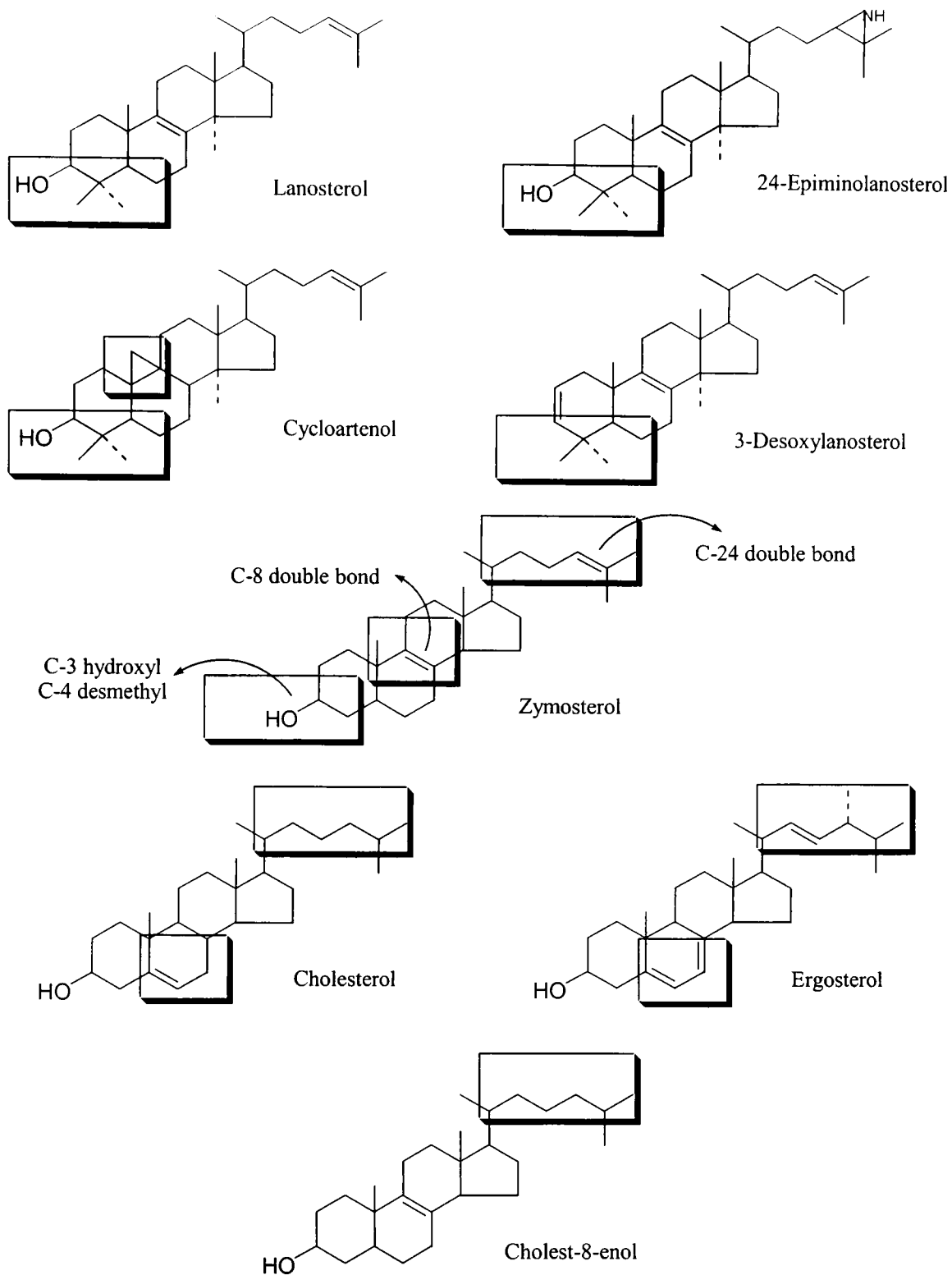


Figure 4.3. Sterol substrates of the yeast SMT with structural features highlighted.

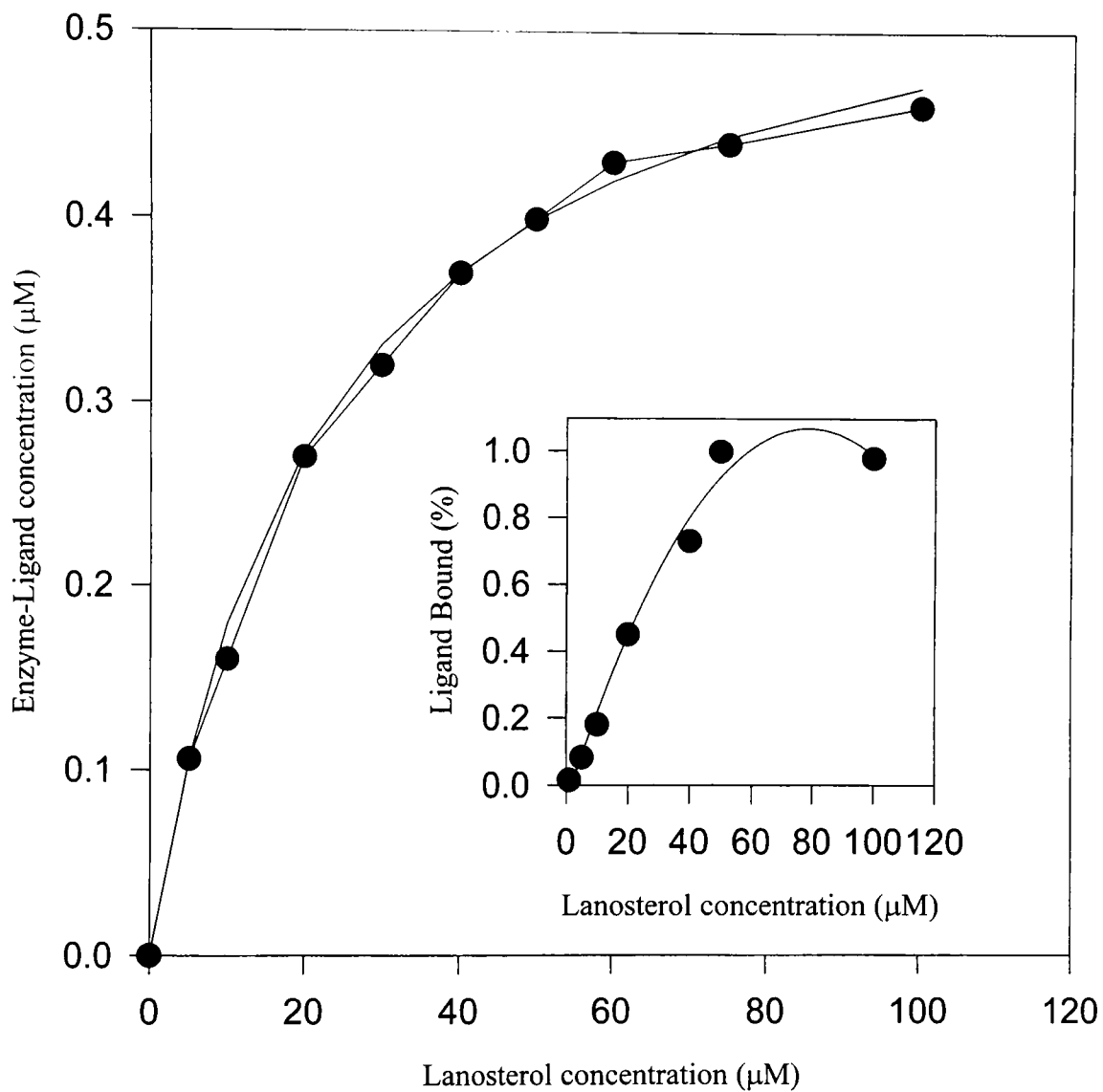


Figure 4.4. Binding isotherm for the native SMT in the presence of increasing lanosterol concentration. K_d is determined from inset plot at 50% ligand bound to the enzyme. Percentage bound is calculated from radioactive counts.

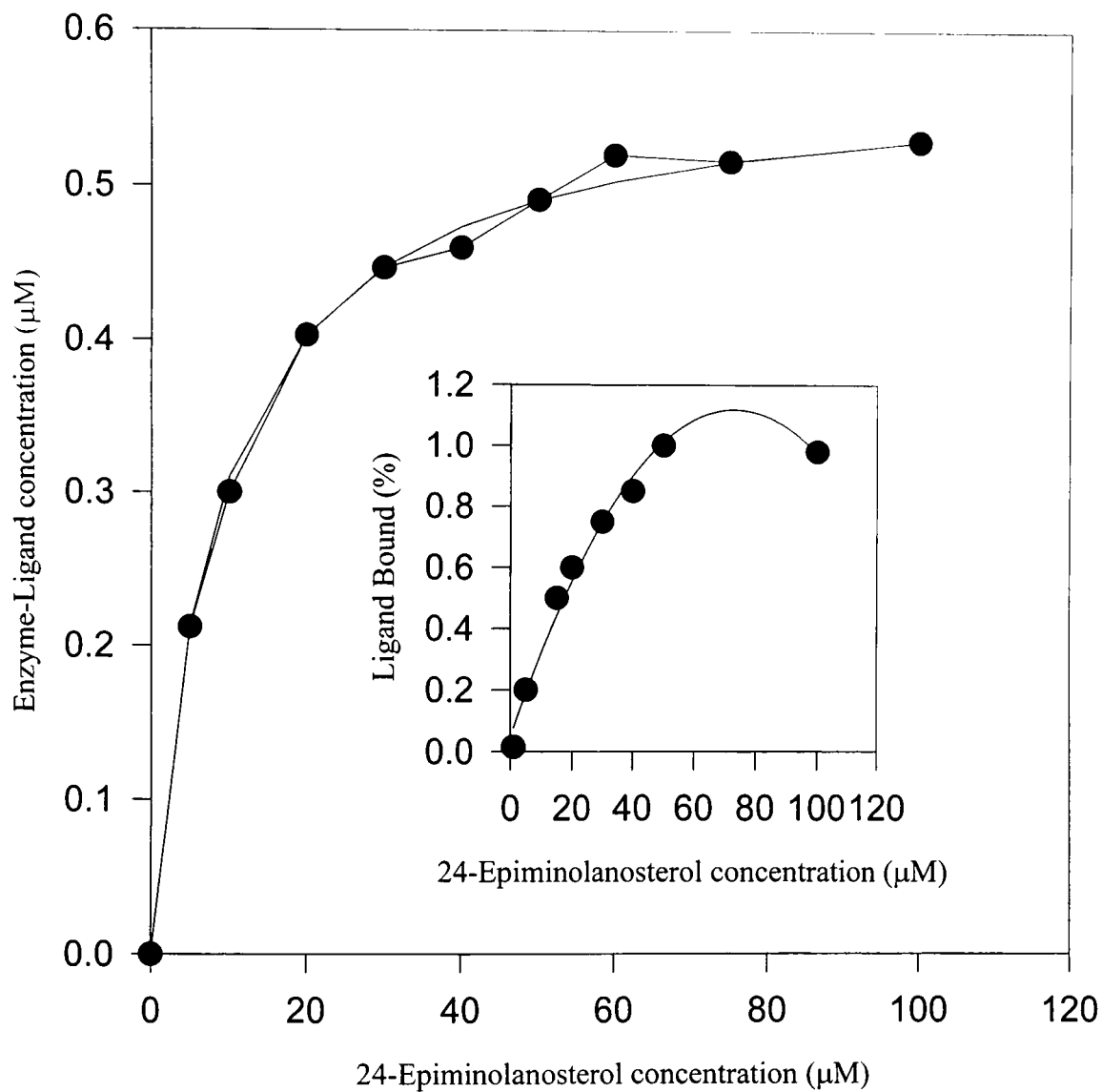


Figure 4.5. Binding isotherm for the native SMT in the presence of increasing 24-epiminolanosterol concentration. K_d is determined from inset plot at 50% ligand bound to the enzyme. Percentage bound is calculated from radioactive counts.

Table 4.1: Steps in the purification of the recombinant yeast SMT.

Fractionation Step	Total Protein (mg)	Total Activity (dpm)	Specific Activity (dpm/mg)	Recovery (%)
Crude Homogenate	4140	621,000	150	100
10,000g supernatant	3111	472,872	152	76
100,000g supernatant	2276	343,676	151	55
0-60% precipitation	2000	314,000	157	51
Q-Sepharose	375	93,750	250	15
ω -Aminodecyl agarose	109	66,817	613	11
Mono Q	80	64,000	800	10

Table 4 2: Dissociation constants for substrates of the yeast SMT and the corresponding calculated Gibb's free energy of binding.

Substrates ¹	K _d (moles)	ΔG (kJ)
1 Zymosterol	4.3 x 10 ⁻⁶	-31.3
2 Fecosterol	3.5 x 10 ⁻⁶	-31.8
3 AdoMet	4.6 x 10 ⁻⁶	-31.1
4 Lanosterol	2.2 x 10 ⁻⁵	-27.2
5 24-Epiminolanosterol	8.5 x 10 ⁻⁶	-29.6
6 3-Desoxylanosterol	7.6 x 10 ⁻⁵	-24.0
7 Ergosterol	7.5 x 10 ⁻⁶	-29.9
8 Cycloartenol	2.5 x 10 ⁻⁵	-26.8
9 Cholesterol	1.6 x 10 ⁻⁵	-28.0
10 Cholesta-8-enol	2.6 x 10 ⁻⁵	-26.7

Note: ¹ The numbers correspond to the structures on Figure 2.1, p. 26.

CHAPTER V

ACTIVE SITE MAPPING

Affinity Labeling of the SMT Sterol Binding Site

An affinity label, or active site directed irreversible inhibitor, is a chemically reactive compound that is designed to resemble a substrate of an enzyme, so that it binds specifically to the active site. This irreversible inhibitor can form a covalent bond with the protein residue during the natural transformation of the substrate to a *C*-methyl product. First, the sterol specificity of the SMT must be established, then an appropriate mechanism-based inactivator may be prepared based on the structure of the substrate. In the yeast SMT, zymosterol was determined to be the preferred substrate for binding whereas lanosterol did not bind productively. Thus, 26,27-dehydrozymosterol (DHZ, 24-cyclopropylidene zymosterol, Figure 5.1) and its corresponding radiolabeled 3-tritio derivative were prepared and assayed with the yeast SMT.

Two outcomes are possible from incubation with DHZ; the inhibitor can be converted to product thereby allowing the enzyme to carry out a normal catalytic cycle, or the inhibitor can form a covalent bond with the protein thereby killing the protein (Figure 5.2). It is possible to distinguish between the 2 outcomes by a combination of kinetic and chemical methods, including the characterization of products released from the enzyme by saponification. The investigator demonstrated the inhibitor could form a covalent bond with the SMT protein in 3 ways. First, the yeast SMT was assayed in the presence of zymosterol and DHZ. Increasing the amount of zymosterol in the assay

mixture afforded protection against inactivation of the enzyme by DHZ. Second, inhibition kinetics revealed that the inhibition was competitive and time-dependent ($K_i = 1.1 \mu\text{M}$, $k_{\text{inact}} = 1.52 \text{ min}^{-1}$, Figure 5.3) Third, a radiolabeled sample of the inhibitor was prepared as described in the Chapter II. The enzyme-inhibitor complex was loaded onto a SDS-PAGE gel and stained with Coomassie blue. The gel was dried and exposed to film for 1 week. The developed film and corresponding gel are shown in Figure 5.4. The film shows the presence of only 1 radioactive band for the enzyme-inhibitor even though other protein bands are present on the gel.

Further insight into catalysis has come from the chemical affinity labeling of the active site of the pure yeast SMT with $[3\text{-}^3\text{H}]$ DHZ. The protein-inhibitor adduct was subjected to cleavage with trypsin and the resulting covalently modified peptide was analyzed by Edman sequencing from the N-terminus. The radiochemically labeled ca. 5.0 kDa peptide fragment of the cleavage mixture was shown to be contiguous through 17 residues to a segment that includes a highly conserved hydrophobic motif unique to SMT enzymes, that is referred to as Region I. Kagan and Clarke (1994) identified several conserved amino acid regions characteristic of AdoMet-dependent methyl transferases, including an AdoMet-binding site and a nucleotide binding site. These conserved motifs are contained in the SMT amino acid sequences. The aligned amino acid sequences corresponding to the sterol binding site contained within the tryptic digest fragment is shown in Figure 5.5. Radioactive counts corresponding to individual residues as isolated from the Edman sequencer is shown in Figure 5.6. Multiple sequence alignment of these SMTs reveals that the proteins show homology of hydrophobic amino acids in Region I.

Based upon these results, the investigator proposed that the sterol docks into a hydrophobic, aromatic-rich pocket of SMT with at least 1 of these aromatic amino acids interacting directly with the sterol C-3 hydroxyl group via hydrogen-bonding interactions (Venkatramesh et al., 1996). The recent three-dimensional structure of a sterol carrier protein has been characterized with ergosterol docked into the sterol binding site with hydrogen-bonding between ergosterol and a tyrosine residue (Boissy et al., 1999).

Affinity Labeling of the AdoMet Binding Site

AdoMet is the methyl donor for the alkylation of sterols as well as other biomolecules including DNA, lipids, and proteins. In 1999, Niewmierzycka and Clarke reported that a large class of AdoMet-dependent-methyltransferases share conserved motifs that interact with a common cofactor, AdoMet. The structures of 9 methyltransferases have been solved that show a similarity in tertiary structure with a similar folding pattern of central parallel β -sheet surrounded by α -helices. The relatedness of the structure is reflected in the amino acid sequence of the conserved motifs in the methyltransferases. The predominant AdoMet binding motifs have been shown to be approximately on the same position on the proteins and at comparable integrals. The motif related to AdoMet binding spans amino acids 124 to 133 in the yeast SMT and is conserved throughout a variety of methyltransferases from many different organisms. From the crystal structure of the Glycine N-Methyltransferase (Fu et al., 1996), the investigators noticed that the binding position of AdoMet was remarkably similar to other methyltransferases. From the known conserved amino acid domains, the

Region I labeling results, and related crystal structures a partial model of the yeast SMT was developed in collaboration with Janusz Bujnicki of the Bioinformatics Laboratory, International Institute of Molecular and Cell Biology, Warsaw, Poland. The active center pocket encompassing Regions I and II along with the structures of the co-substrates are shown in Figure 5.7.

AdoMet has been shown to specifically label methyltransferases using high intensity short wave UV irradiation. The covalent linkage formed between the protein and AdoMet allows for proteolytic digestion and isolation of peptides bound to the substrate. Based upon the protocol reported by Subbaramaiah and Simms (1992) and discussed in Chapter II the AdoMet binding site was mapped. First, an experiment was done varying the time of irradiation with activity of the SMT. AdoMet and SMT were incubated under UV light and then assayed in the presence of zymosterol. As time of irradiation increased, conversion of zymosterol to product decreased (Figure 5.8). Second, the linked [^3H] AdoMet-SMT complex was subjected to electrophoresis by SDS-PAGE. The gel was dried and then exposed to film for 2 weeks. The developed film showed a band corresponding to the migration of the yeast SMT. The radiolabeled AdoMet formed a covalent link to the SMT as shown in Figure 5.9.

The protein-AdoMet adduct was subjected to cleavage with trypsin and the resulting covalently modified peptide was isolated by reverse phase HPLC. The fractions were counted and radioactivity plotted versus fraction time. The results are shown in Figure 5.10 indicated the radiolabeled peptide adduct. Non-radioactive AdoMet-SMT tryptic fragments isolated according to the established HPLC protocol were analyzed by

Edman sequencing from the N-terminus. The labeled ca. 15.0 kDa peptide fragment of the cleavage mixture was shown to be contiguous through 23 residues to a segment that includes a highly conserved hydrophobic motif unique to SMT enzymes, that is referred to as Region II. The aligned amino acid sequences corresponding to the AdoMet binding site contained within the tryptic digest fragment is shown in Figure 5.11. The covalently linked tryptic digest fragment was sent to the Scripps Biotechnology Institute for analysis by MALDI-TOF mass spectrometry. The result of analysis is shown in Figure 5.12.

Site Specific Mutagenesis of Regions I and II

Due to the relationship between the conserved motifs in AdoMet-dependent-methyltransferases and the related structure of the protein, site-directed mutagenesis is a viable tool to probe the structure-function relationships in the active site of the yeast SMT. In 1996, Ahmad and Rao stated that mutations of amino acids in the conserved sequence of Region II disrupted AdoMet binding but left the second substrate's binding (in this case DNA) unaltered. Roth, Helm-Kruse, Friedrich, and Jeltsch (1998) reported that the amino acid sequence in Region II appears to be significant in AdoMet binding and specific residues could contribute to catalysis and/or specific interactions with AdoMet. Thus, the investigator decided to probe conserved amino acids in Regions I and II that when mutated would disrupt zymosterol and/or AdoMet binding. If Region I is definitively the sterol binding site then it is reasonable to predict that a mutation of a critical residue that is absolutely conserved would disrupt sterol binding and likewise a mutation of a critical residue would disrupt AdoMet binding in Region II.

As described in Chapter II, routine mutagenesis can be performed using the Direct PCR method. As shown in Figures 5.5 and 5.11, respectively, threonine 78 and proline 133 are absolutely conserved throughout the sequences of related proteins. Threonine contains a hydroxyl in the side chain that may interact with the nucleophilic features of the sterol. Proline is positioned in a key location in the Rossman fold region as demonstrated by related crystal structures. Threonine was changed to valine, which is a nonpolar side chain without any potential hydrogen-bonding features. Proline was changed to leucine, a highly hydrophobic residue that lacks the fused ring of proline. The structures of the amino acid residues are shown in Figure 5.13. After confirmation of the substitution by sequencing, the mutants were checked for activity. Both T78V and P133L were inactive although they could be purified according to standard protocols. Both mutants were investigated for binding potential with each of the substrates, zymosterol and AdoMet. Whereas T78V could bind AdoMet with some efficiency, it was not able to bind zymosterol. Likewise, P133L could bind zymosterol but not AdoMet. The results of these studies are summarized in Table 5.1. Western blots of the 2 mutants were generated with antibody raised against the yeast SMT (Figure 5.14). Both proteins were immunologically related to the native SMT. The tyrosine-81 to phenylalanine mutant was also tested as a control (more discussion will follow in Chapter VI regarding the importance of this residue) and the results given in Table 5.1. The mapping results discussed in this chapter identify Region I as the sterol binding site and Region II the AdoMet binding site.

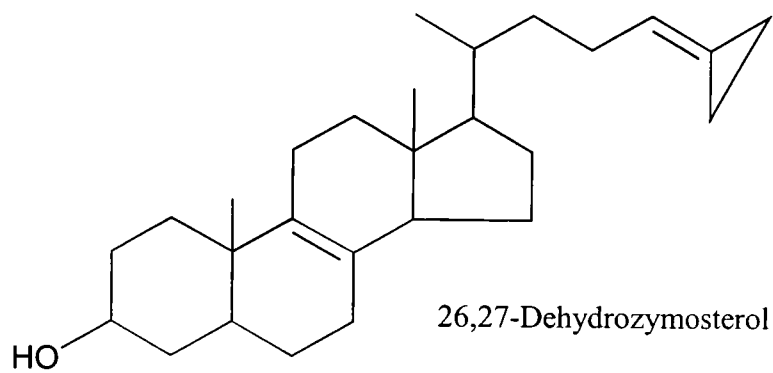


Figure 5.1. The structure of 26,27-dehydrozymosterol (24-cyclopropylidene zymosterol).

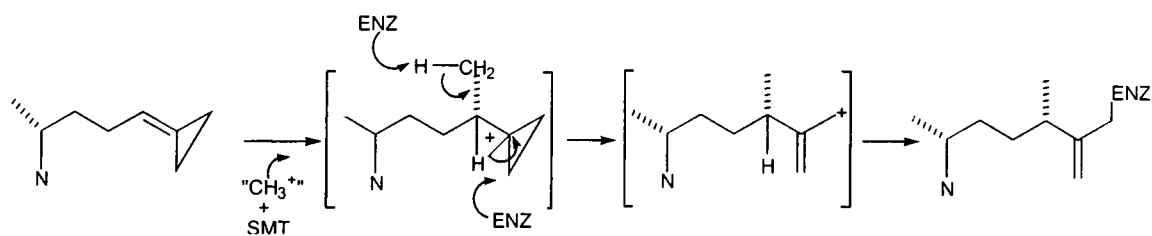


Figure 5.2. The scheme shows the proposed mechanism of inactivation of the SMT enzyme by 26,27-dehydrozymosterol. “N” represents the zymosterol nucleus.

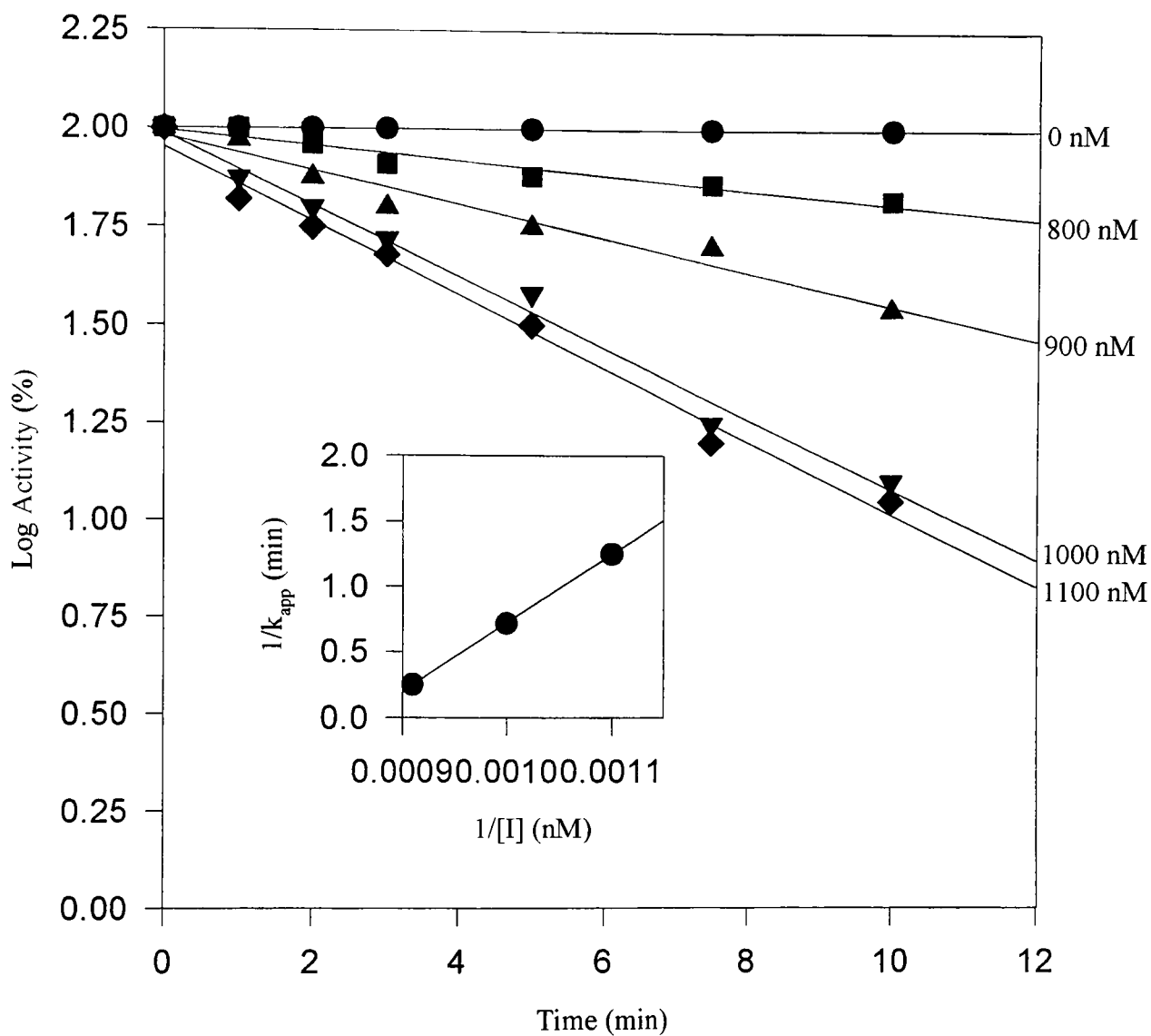


Figure 5.3. Time dependent inactivation of the yeast SMT with 26,27-dehydrozymosterol. Inset graph is a replot of apparent rate at log 50% activity versus $1/\text{inhibitor concentration}$ (Marshall, 1998).

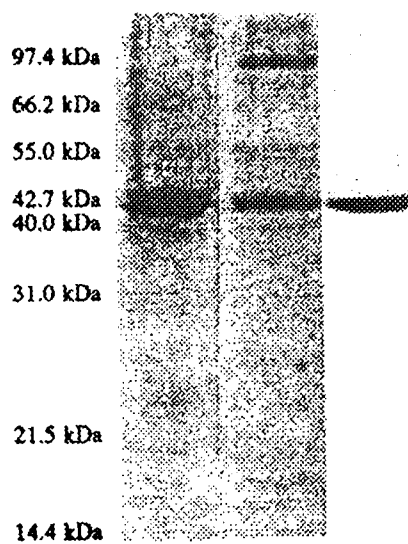


Figure 5.4. SDS-PAGE and corresponding film of the SMT-26,27-dehydrozymosterol adduct. Lane 1 is the SDS-PAGE of the unlabeled protein; lane 2 is the 26,27-dehydrozymosterol labeled protein; and lane 3 is the corresponding film of the labeled protein at 43 kDa (Marshall, 1998).

Tryptic Digest

	<u>Region I</u>			
62	1 R L E D Y N E A T H S Y Y N V V T D F Y E Y G W G S S F H F S R F Y K G E S F A A S I A R	78	91	106
2	2 T D F Y E Y G W G S S F H F			
3	3 T D L Y E Y G W S Q S F H F			
4	4 T S F Y E Y G W G E S F H F			
5	5 T S F Y E Y G W G E S F H F			
6	6 T S F Y E F G W G E S F H F			
7	7 T S F Y E F G W G E S F H F			
8	8 T D I Y E W G W G Q S F H F			
9	9 T S F Y E Y G W G E S F H F			
10	10 T S F Y E Y G W G E S F H F			
11	11 T S F Y E Y G W G E S F H F			
12	12 T D I Y E Y G W G Q S F H F			
13	13 T D I Y E W G W G Q S F H F			
14	14 T S F Y E F G W G E S F H F			
15	15 T D T Y E W G W G Q S F H F			
16	16 T D I Y E W G W G Q S F H F			
17	17 T S F Y E Y G W G E S F H F			
18	18 T D T Y E W G W G Q S F H F			
19	19 T S F Y E Y G W G E S F H F			

Figure 5.5. Amino acid composition of Region I from several SMTs (referenced to Genbank numbers) aligned against the tryptic fragment from *S.cerevisiae* including Region I: 1, X74249, *S. cerevisiae*; 2, AF031941, *C. albicans*; 3, SPBC16E9, *S. pombe*; 4, AF045570, *Z. mays*; 5, ZMU79669, *Z. mays*; 6, U43683, *G. max*; 7, AF042332, *O. sativa* I; 8, AF042333, *O. sativa* II; 9, U60754, *T. aestivum*; 10, U81312, *N. tabacum* I; 11, AF053766, *N. tabacum* II; 12, U71108, *N. tabacum* III; 13, NTU71107, *N. tabacum*; 14, U81313, *R. communis*; 15, AF195648, *A. thaliana* I; 16, U771400, *A. thaliana* II; 17, X89867, *A. thaliana* III; 18, ATU71400, *A. thaliana*; 19, TAU60755, *T. aestivum*.

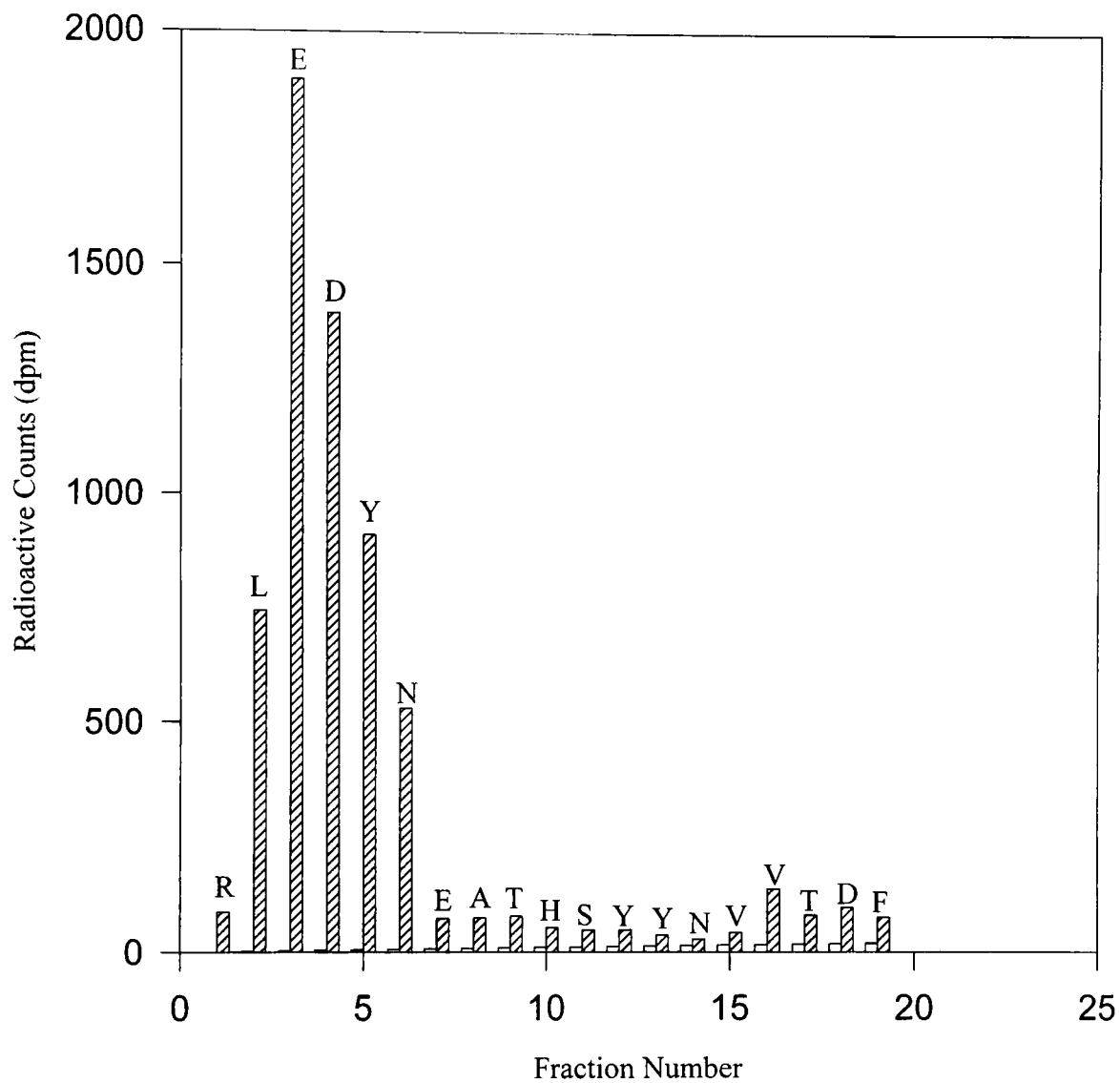


Figure 5.6. Radioactive counts of individual fractions corresponding to the amino acid residues sequenced in Region I.

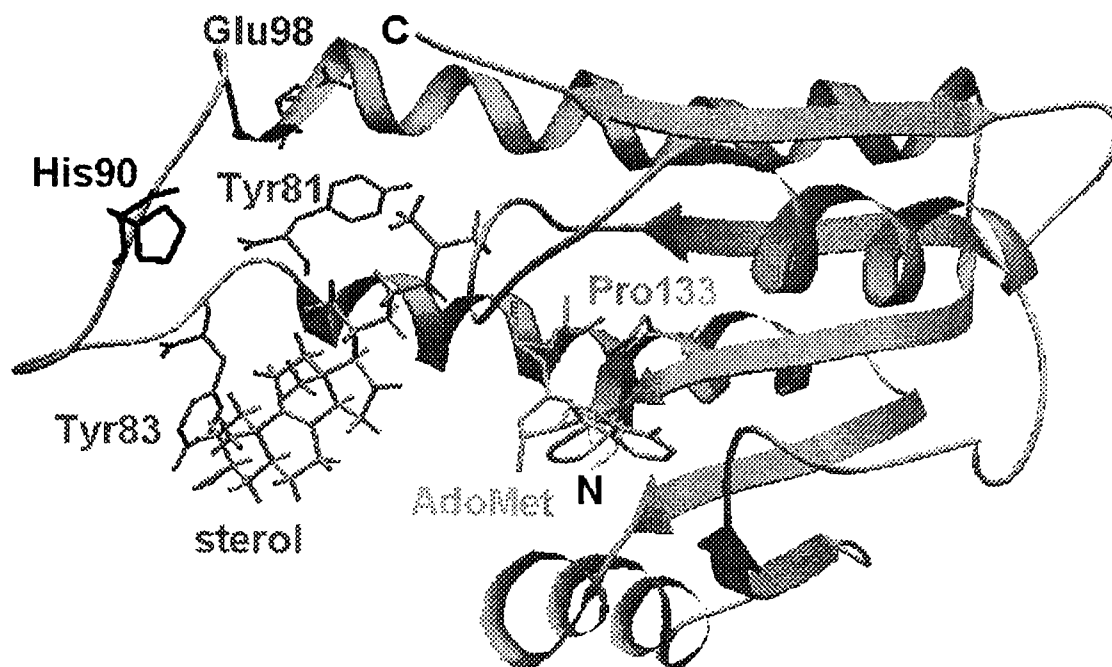


Figure 5.7. Theoretical model of the yeast SMT active site pictured with the co-substrates, ergosterol and AdoMet. We thank Janusz Bujnicki for providing this secondary structure prediction of the SMT.

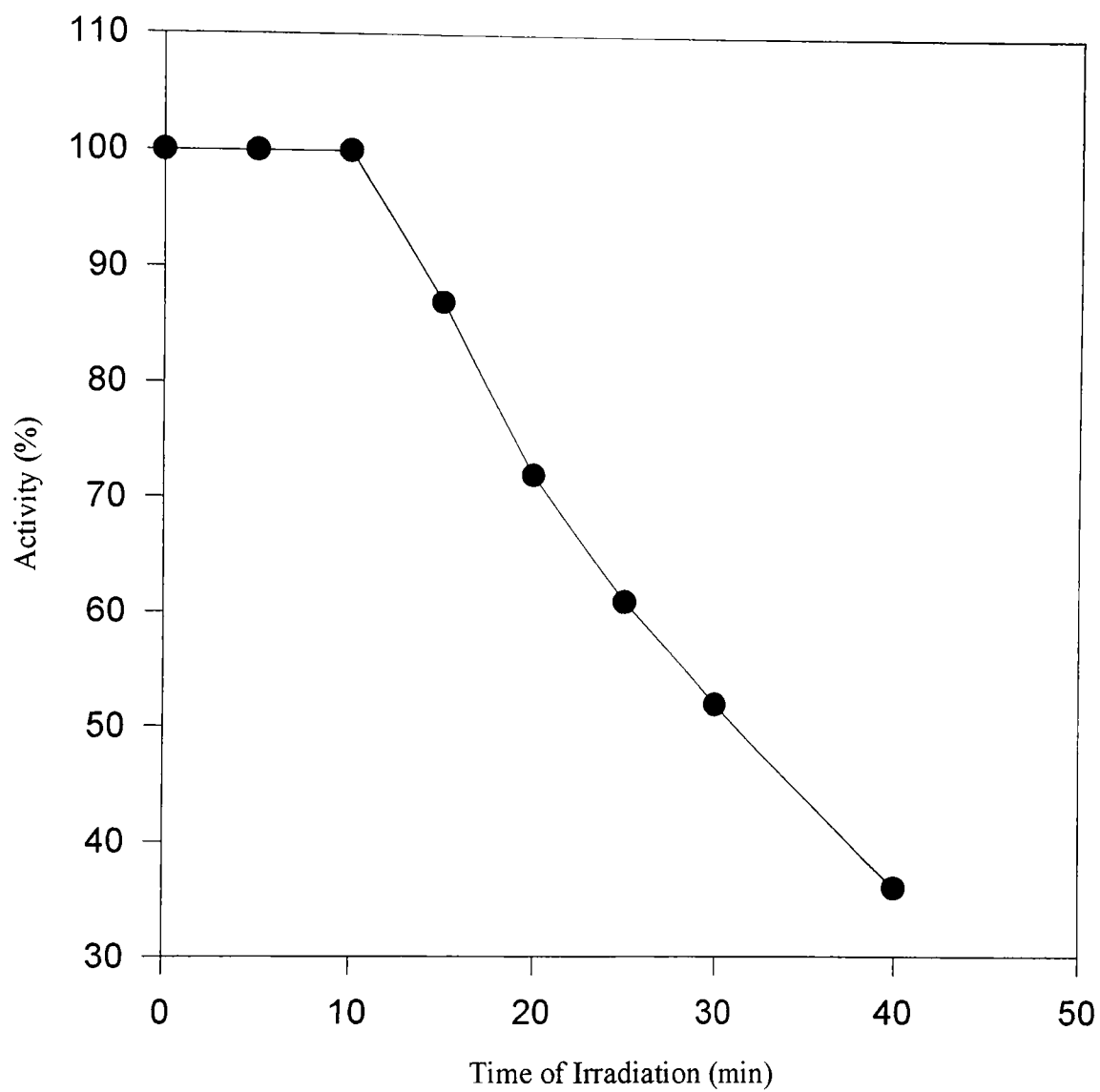


Figure 5.8. Percent SMT activity remaining versus time of UV irradiation of SMT and AdoMet at 254 nm.



Figure 5.9. SDS-PAGE and corresponding film of the SMT-AdoMet adduct. Lane 1 is the SDS-PAGE of the SMT complexed with AdoMet and lane 2 is the corresponding film.

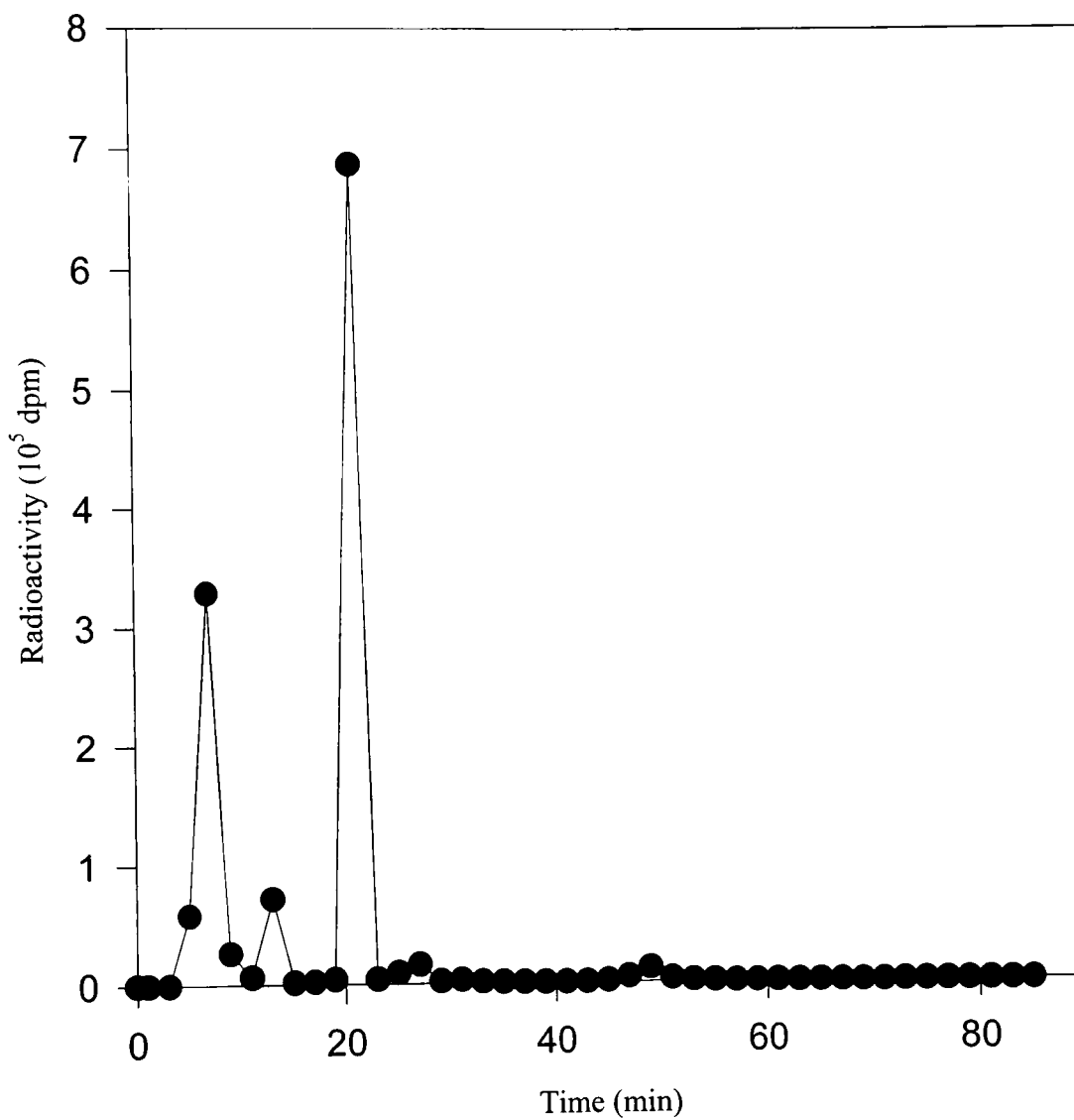


Figure 5.10. Radioactive counts of the fractions collected from the HPLC purification of the complexed SMT-AdoMet tryptic peptides versus time of fraction collection.

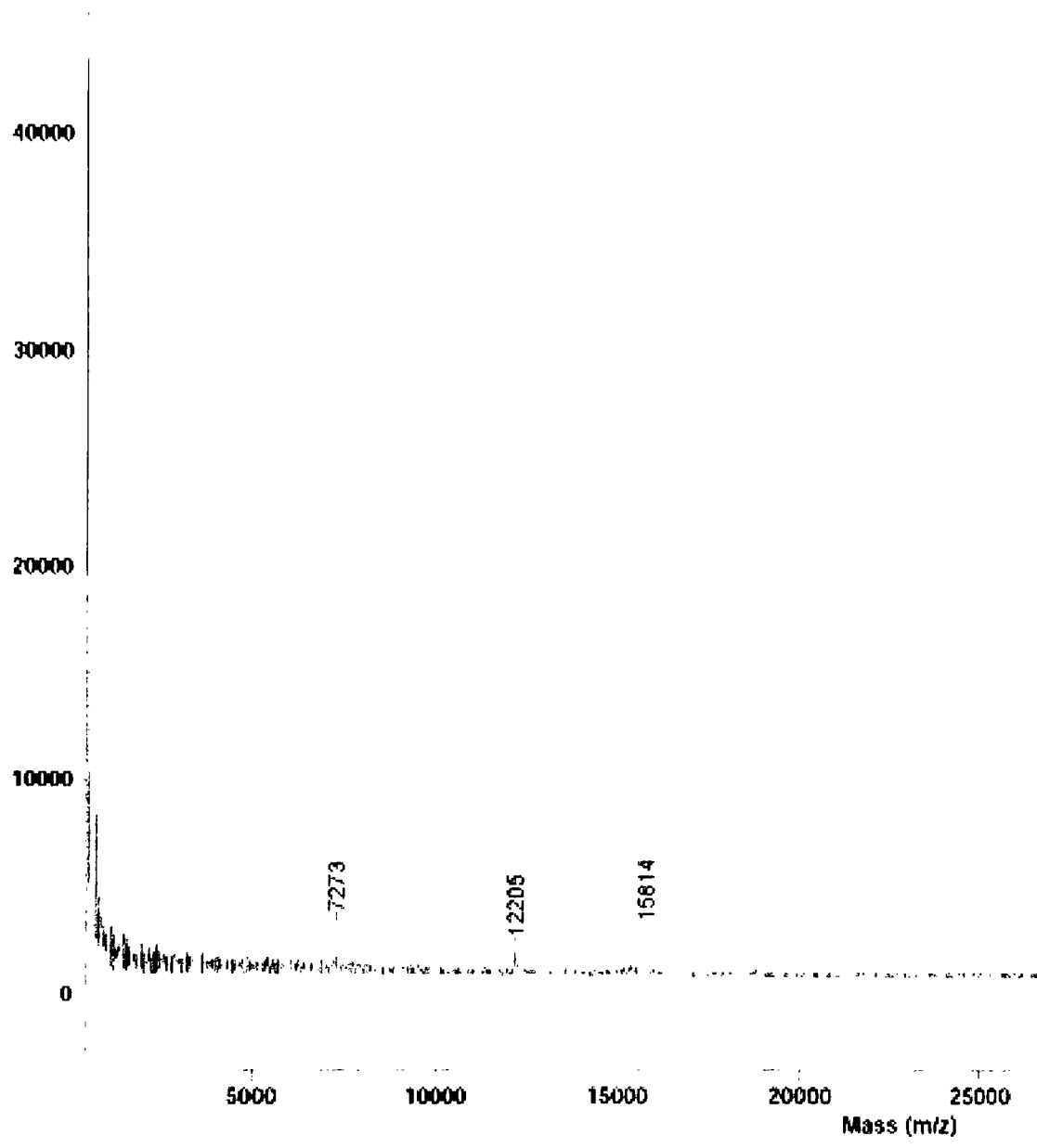


Figure 5.12. MALDI-TOF analysis of the tryptic digested AdoMet-SMT complex.

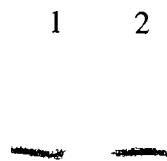


Figure 5.14. The Western blot of the yeast mutants, P133L (lane 1) and T78V (lane 2). The blots were obtained using antibody raised against the native yeast SMT. Both blots correspond to protein bands migrating at 43kDa as determined from SDS-PAGE marker.

Table 5.1: Equilibrium binding constants and catalytic competence for the native SMT and 3 selected mutants from Region I and II

Protein Source	Zymosterol K_d (μM)	AdoMet K_d (μM)	Zymosterol k_{cat} (s^{-1})
Wild Type	4.3	4.6	10.9×10^{-3}
Y81F	4.3	4.6	10.9×10^{-3}
T78V	--	9.2	NA
P133L	15.0	--	NA

CHAPTER VI

SITE SPECIFIC MUTAGENESIS OF TYROSINE 81

From the parent yeast SMT, a series of mutants were constructed by site-directed mutagenesis at position 81, which is absolutely conserved for aromatic amino acids in the sterol binding site (Region I, Figure 5.5). The tyrosine residue was changed to phenylalanine, tryptophan, leucine and alanine (Figure 6.1). These amino acids were systematically modified and the resulting mutant proteins overexpressed in *E. coli* and purified to homogeneity (Nes et al., 1999). The mutant SMTs were found to be similar to the native protein in chromatographic behavior and organization as indicated by the MALDI-TOF mass spectra shown in Figures 6.2 (Y81F) and 6.3 (Y81W). The Scripps Institute in La Jolla generated the Y81W MALDI from a purified sample sent to them by the investigator. The mutant series reacted positively in immunoblot analysis with polyclonal antibodies raised against the native yeast SMT (Figure 6.4).

Kinetic Isotope Effects

The Y81F mutant gave unnatural behavior as indicated by the remarkable change in substrate specificity and product distribution compared with that observed earlier for the wild-type protein (Nes et al., 1999). Whereas the K_m and k_{cat} determined for zymosterol was the same for the mutant as for the wild-type SMT, the mutant catalyzed 4 α -methyl zymosterol that the wild-type failed to catalyze. The mutant also transformed the product of zymosterol catalysis, fecosterol, to three 24-ethyl products with the

$\Delta^{24(28)}E$ -, $\Delta^{24(28)}Z$ - and 24β -ethyl side chain structures which the wild-type enzyme also failed to do. The mutant fungal SMT was acting much like a plant SMT exhibiting multiple activities.

Changes in rate of C-methylation and product distribution resulting from deuterium substitution at C-28 were used to establish the kinetic isotope effects (KIEs) for the various deprotonations leading to the 24-methylene, 24-ethylidene, and 24-ethyl sterols. An isotope effect on C-28 methyl deprotonation generated during the first C_1 -transfer was detected with zymosterol or desmosterol paired with AdoMet or [2H_3 -methyl]AdoMet. A similar experiment to test for a KIE generated during the second C_1 -transfer reaction with AdoMet paired with 24(28)-methylene cholesterol or [2H_2]24(28)-methylene cholesterol indicated an inverse isotope effect associated with C-27 deprotonation. Alteration in the proportion of the C-24 alkylated olefinic products generated by the pure Y81F mutant resulted from the suppression of the formation of $\Delta^{24(28)}$ -ethylidene sterols (C-28 deprotonation) by a primary deuterium isotope effect with a compensating stimulation of the formation of the 24-ethyl sterols (C-27 deprotonation). From the structures and stereochemical assignments of the C-ethyl olefin products, the stereochemistry of the attack of AdoMet in the second C_1 -transfer was found to operate a *Si*-face (backside) attack at C-24, analogous to the first C_1 -transfer reaction. The complement of C_1/C_2 -activities characterized in the Y81F mutant is much the same as that in the soybean SMT.

Equilibrium Dialysis and Kinetic Experiments

C-methylation of the sterol side chain has been examined further by comparing the activity of the wild-type enzyme with a series of position-81 mutants tested against zymosterol and DHZ. First, equilibrium binding constants were determined for each mutant with zymosterol and results shown in Table 6.1. Second, kinetic parameters were determined for each mutant with zymosterol and results shown in Table 6.1 as well. Measurements of K_d and k_{cat} for zymosterol showed that the binding efficacy and rate of transmethylation were affected by the electronics of the sterol side chain and the electron density and steric elements of the residue at position-81. Third, the inhibition kinetics of each mutant with DHZ was measured. IC_{50} for Y81W, Y81F, and Y81L were shown to be 20 μM , 27 μM , and 33 μM , respectively (Figures 6.5, 6.6, and 6.7). The Y81A inhibition pattern was not detectable due to low activity of the enzyme relative to the other mutants. Fourth, the time-dependent inactivation kinetics of the Y81W SMT were found to be a $K_i = 20 \mu\text{M}$ and $k_{inact} = 47 \text{ min}^{-1}$ as compared to the wild-type SMT, $K_i = 1 \mu\text{M}$ and $k_{inact} = 1.5 \text{ min}^{-1}$ (Figure 6.8). The mutagenesis experiments indicate an aromatic amino acid at position-81 can exert control over the binding properties of substrates and promote the reaction pathway to product partitioning that leads to modified inhibitor potency. These differences in molecular recognition can be used to formulate class-selective inhibitor design to impair SMT action in opportunistic infections or phytopathogens.

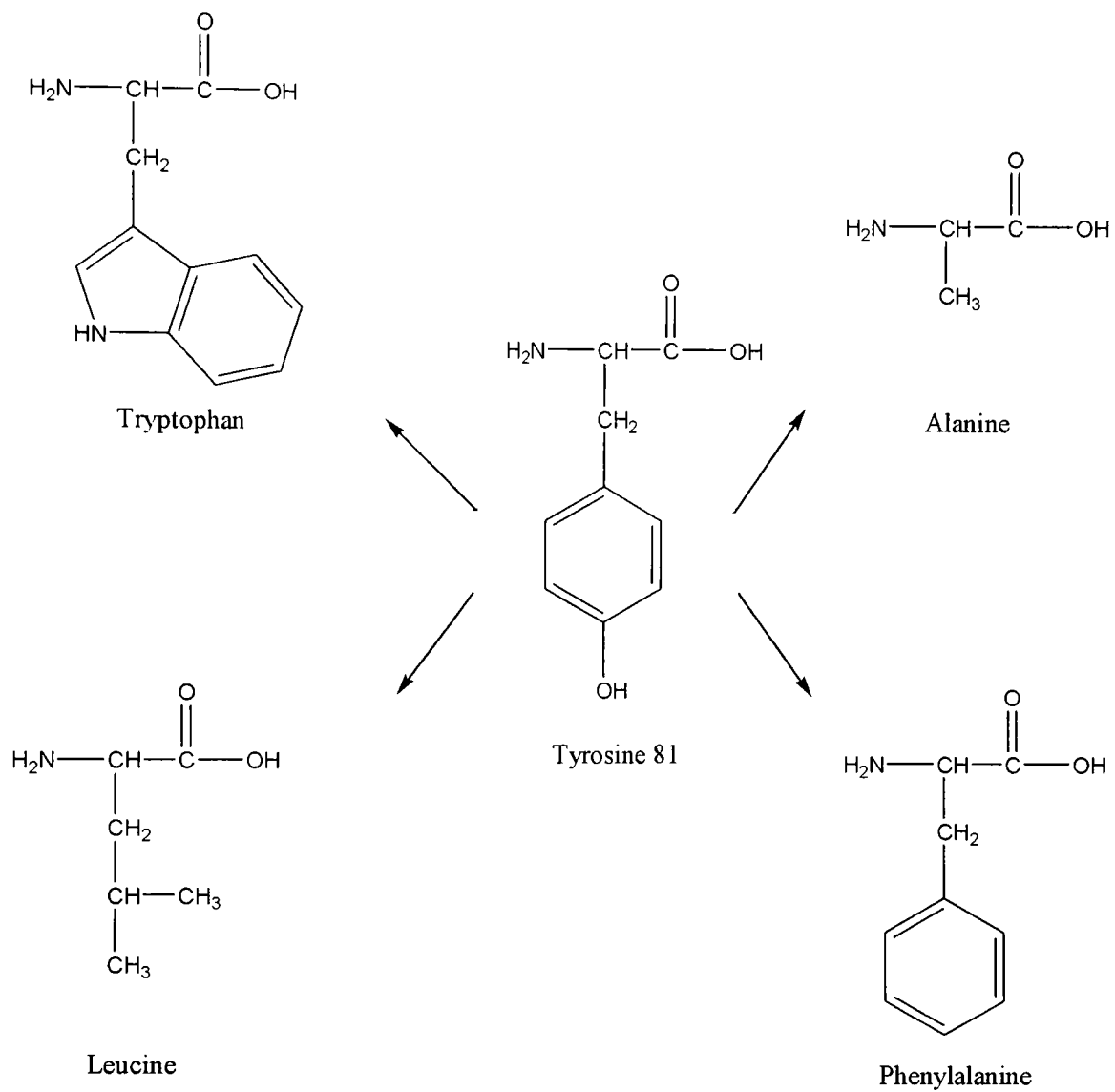
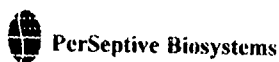


Figure 6.1. Amino acid substitutions in the site-specific Mutagenesis of tyrosine 81.



Inqmat File name: c:\msp\p1\h1\c\file\June1806.ms
File File # 4 = C:\VOYAGER\DATA\AILYLC\JUNE1806.MS

Comment:

Method: LYLCL	Laser: 2250
Accelerating Voltage: 25000	Scans Averaged: 6
Grid Voltage: 60.000 %	Pressure: 2.13e-07
Guide Wire Voltage: 0.300 %	Low Mass Gate: 2000 u
Delay: 500.000	Trigger: 6.000
Sample: 21	Collected: 05/10/00 1:40 PM

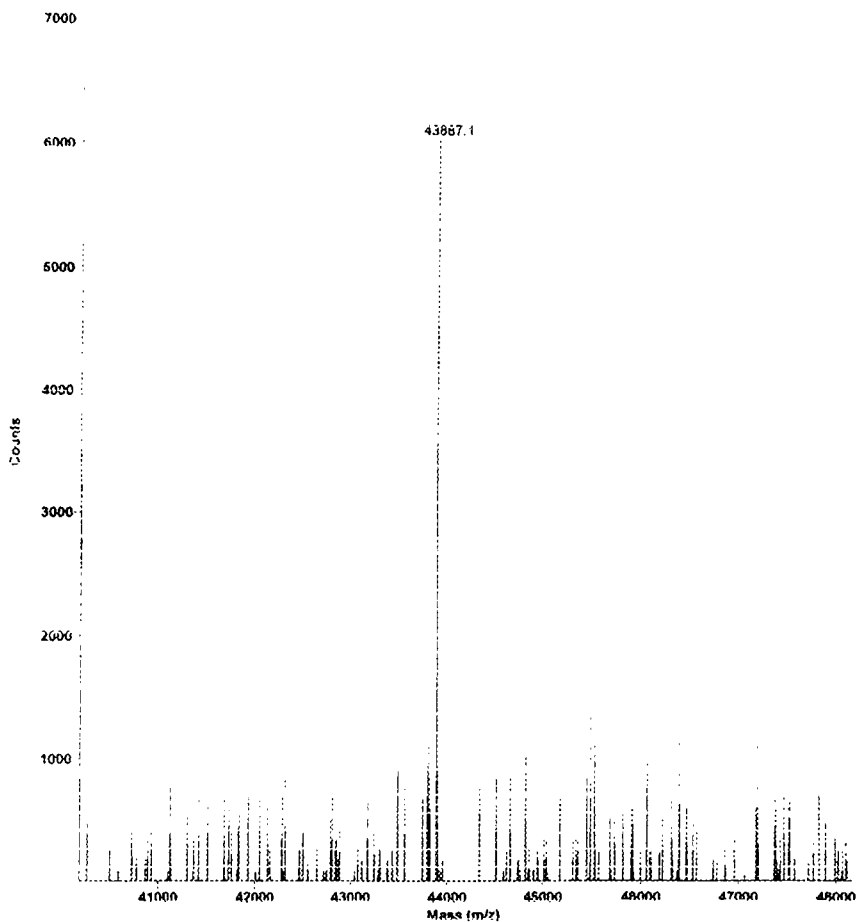


Figure 6.2. MALDI-TOF analysis of the Y81F mutant SMT showing the monomeric molecular weight, 43,887 Da. The mass and chromatographic pattern show this mutant protein to be a SMT species.

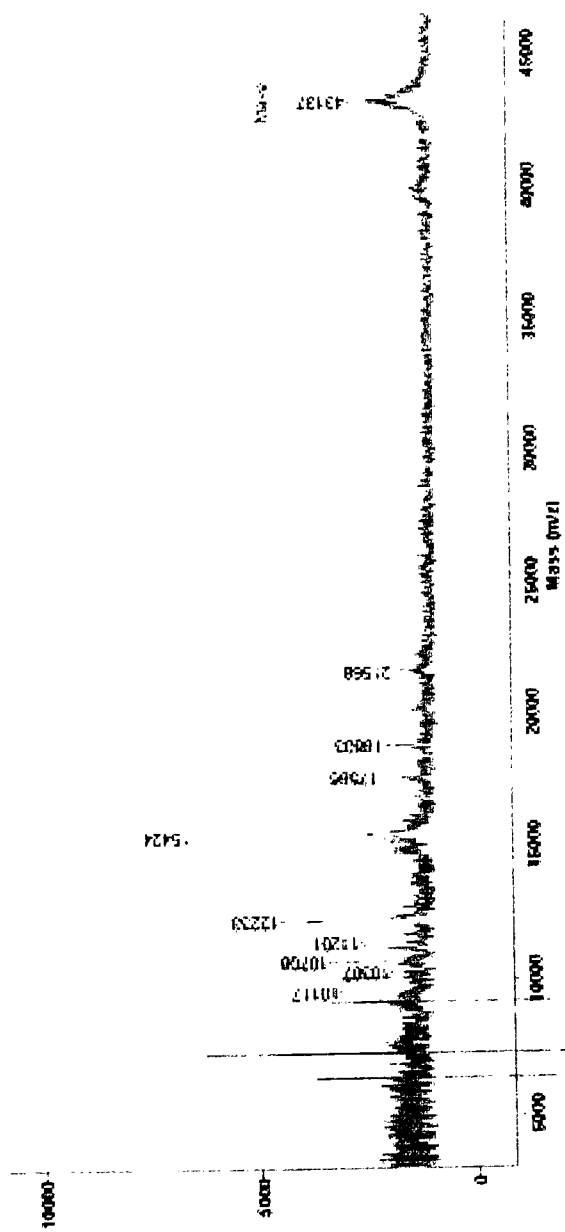


Figure 6.3. MALDI-TOF analysis of the Y81W mutant SMT showing the monomeric molecular weight, 43,137 Da.

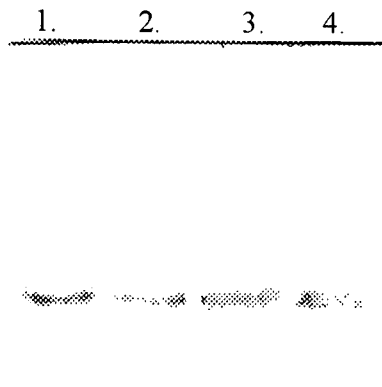


Figure 6.4. Western blot of the yeast mutants, Y81F (lane 1), Y81W (lane 2), Y81L (lane 3), and Y81A (lane 4). The blots were obtained using antibody raised against the native yeast SMT. The bands shown correspond to protein bands migrating at 43 kDa as determined from SDS-PAGE.

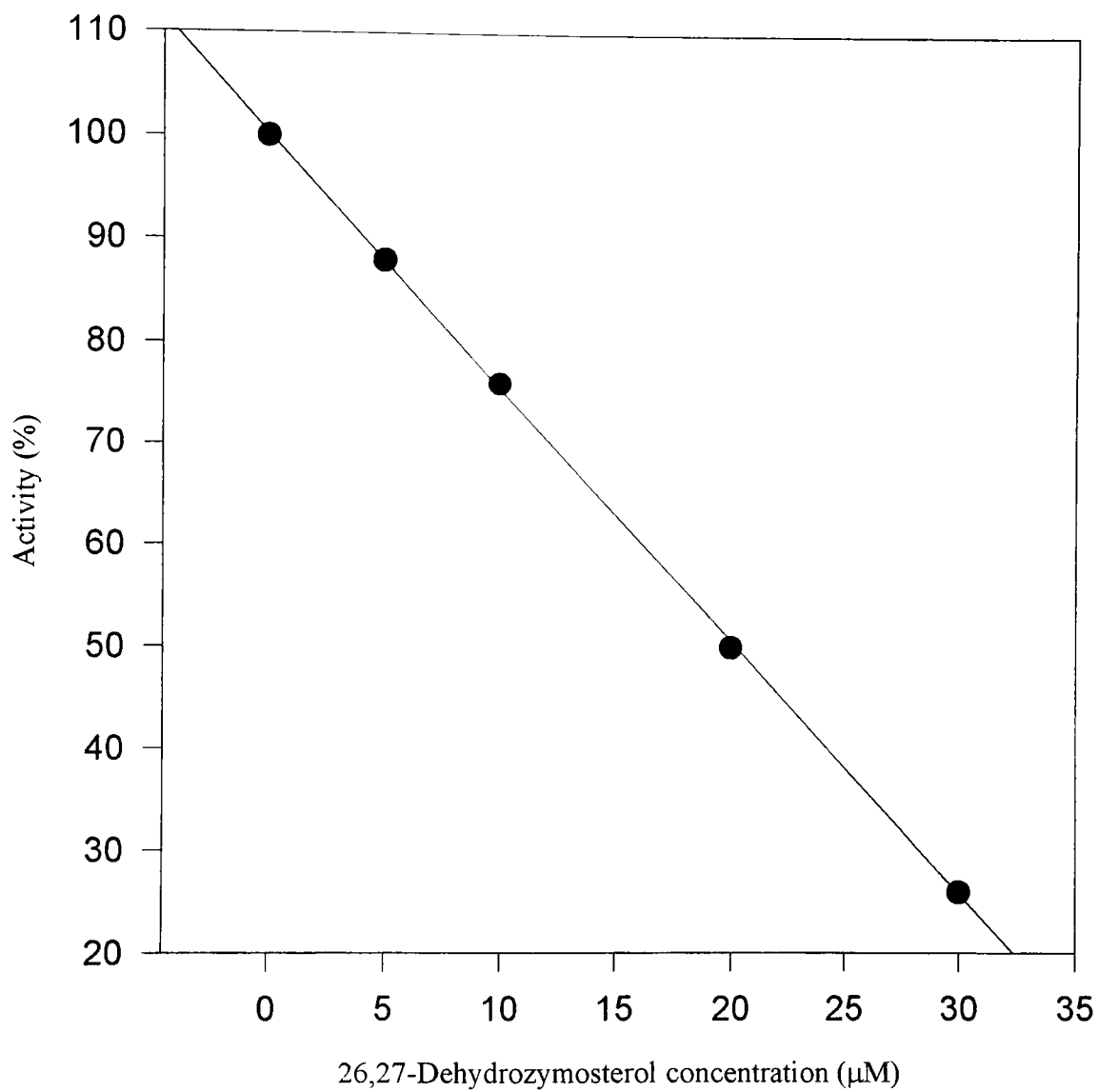


Figure 6.5. Inhibition plot for the Y81W mutant SMT with 50 μM zymosterol and increasing 26,27-dehydrozymosterol.

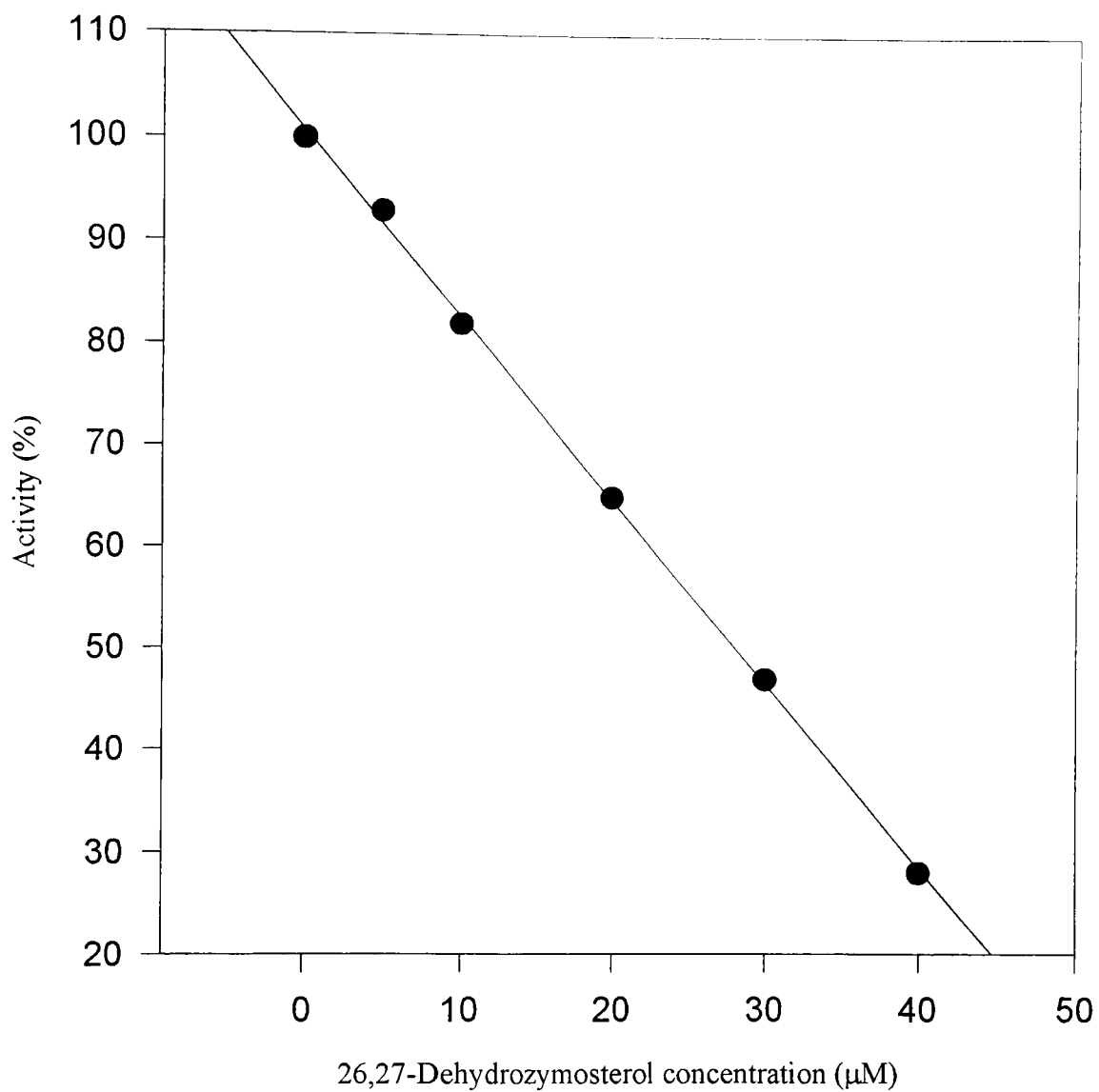


Figure 6.6. Inhibition plot for the Y81F mutant SMT with 50 μM zymosterol and increasing 26,27-dehydrozymosterol.

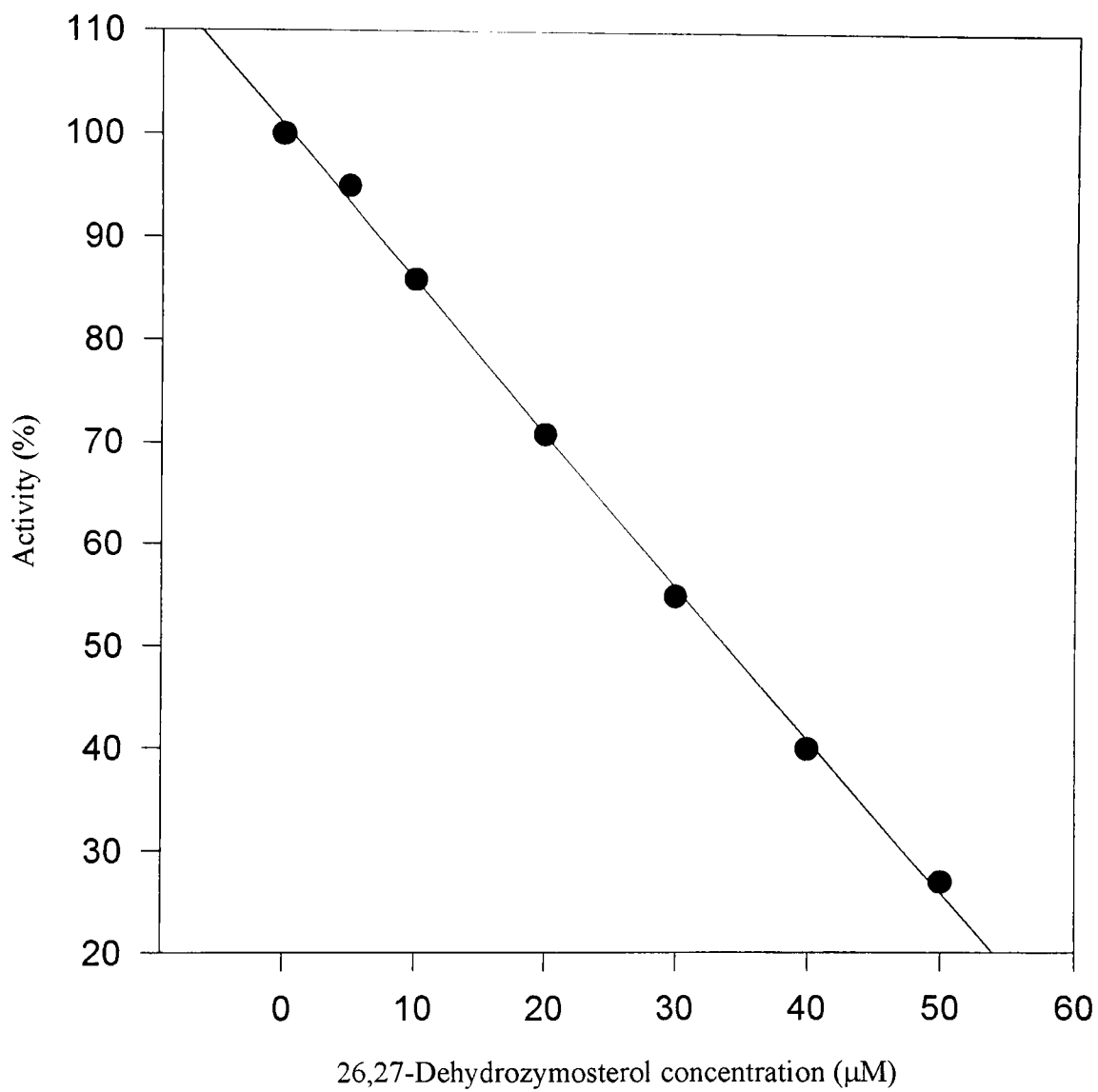


Figure 6.7. Inhibition plot for the Y81L mutant with 50 mM zymosterol and increasing 26,27-dehydrozymosterol.

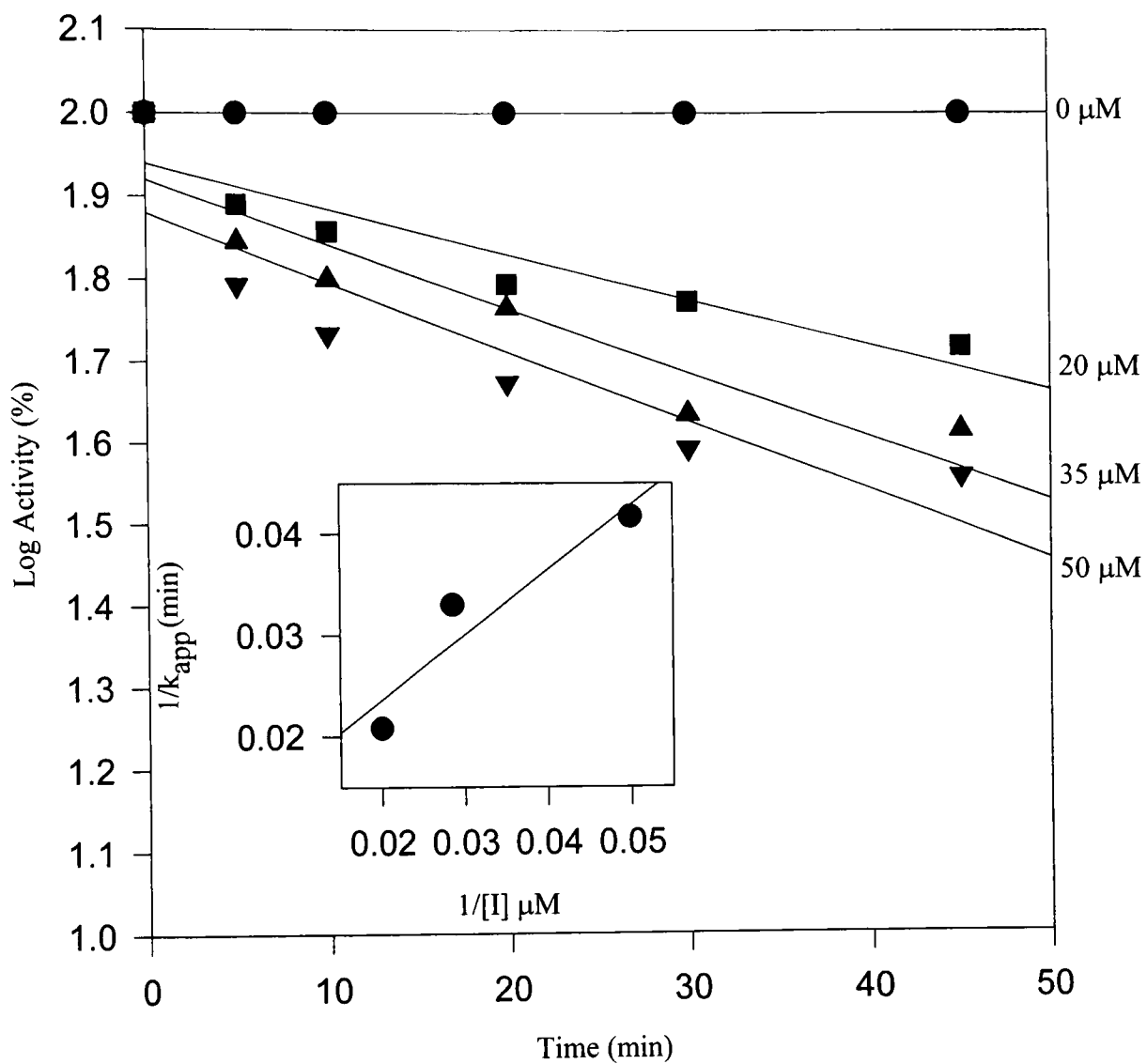


Figure 6.8. Time dependent inactivation of the Y81W mutant SMT with 26,27-dehydrozosterol. Inset graph is a replot of apparent rate at log 50% activity versus 1/inhibitor concentration.

Table 6.1: Kinetic and equilibrium dialysis results for the native SMT and Y81 series with zymosterol and 26,27-dehydrozymosterol (DHZ). (Y- tyrosine, W- tryptophan, L- leucine, A-alanine).

Protein	DHZ K_d (μM)	Zymosterol K_d (μM)	Zymosterol K_m (μM)	kcat 10^{-3}s^{-1}	Zymosterol $\Delta\Delta G$ (kJ)
Native	4.0	4.3	12.0	10.9	0.0
Y81W	5.6	9.6	28.0	14.6	0.73
Y81F	9.5	3.5	12.0	10.0	0.17
Y81L	11.0	6.6	4.0	4.5	1.15
Y81A	11.0	8.8	11.0	1.1	1.75

CHAPTER VII

DISCUSSION

On the basis of present understanding of phytosterol biosynthetic relationships, SMT occupies a position as a key branch point enzyme of phytosterol synthesis. The various SMTs in plants and fungi have clearly evolved a similar mechanistic plan, which is reflected in the conservation of genetic material in the active site of these proteins. The mechanism of *C*-methylation involves β -face attack, which can result in product diversity from the same active site as demonstrated in the results from this research program.

First, with the development of an expression and purification system (discussed in more depth in Marshall's Master's thesis, 1998) it was possible to study the catalytic and binding efficiency for a variety of sterol substrates, intermediates as well as end products. Using a recombinant protein, catalytic competence and product partitioning was investigated giving rise to the features of the sterol necessary for catalysis by the yeast SMT. The equilibrium binding constants were determined for a variety of substrates in the absence of catalysis or influence by the co-substrate, AdoMet. The results are interpreted to imply that *C*-methylation of sterol substrates is not entirely dependent on the binding efficacy of the sterol although some features (i.e., C3-hydroxyl) are clearly important in positioning the sterol in the active site. The conversion of particular sterols seems to be most affected by the orientation of steroid nucleus and side chain with respect to key amino acids in the active site.

Second, modulators of SMT were investigated including ATP and sterol end products such as ergosterol. In previous discussions by the investigator and collaborators the modulation of SMT by feedback inhibition of sterol end products has been described. However, for the first time a non-sterol compound has been shown to influence not only SMT activity but also the carbon flux of the phytosterol pathway through C₁/C₂ partitioning. The results are interpreted to imply that ATP can influence the branch-point chemical “decisions” of the SMT as a direct consequence of cellular conditions.

Third, the active site of the SMT both sterol and AdoMet binding sites has been mapped. The use of the DHZ affinity label and AdoMet photo labeling has allowed the SMT to be tagged, digested, and sequenced in close proximity to the active site. The mutations in Regions I and II show a relationship in amino acid identity and binding of the co-substrates. Moreover, there is a direct relationship between SMTs and other methyltransferase sequence and structure as expressed by amino acid conservation in specific domains of the enzymes. The kinetic results from the mutation at position 81 in the highly conserved aromatic rich region common to SMTs more specifically address how a small difference in active site topography can influence product partitioning and diversity.

An understanding of the enzymology and regulation of the phytosterol pathway can permit the manipulation of the flux of intermediates to be channeled to the formation of a desirable end product or can lead to changes in the steady-state concentration of intermediate to end product. Comparison of the amino acid sequences and mechanisms should provide clues to the origin and evolution SMT enzymes. For fungi, a series of

rationally designed specific inhibitors will be developed. Further investigation of the pathway through site-specific mutagenesis and x-ray crystallographic analysis can be expected to provide a basis for directed manipulation of the phytosterol pathway.

SELECTED BIBLIOGRAPHY

- Ahmad, I., and Rao, D. (1996) *J. Mol. Biol.* **259**, 229-240.
- Arigoni, D. (1978) *Ciba Found. Symp.* **60**, 243-258.
- Back, K., and Chappell, J. (1996) *Proc. Natl. Acad. Sci.* **93**, 6841-6845.
- Bansal, S.R., and Knoche, H.W. (1981) *Phytochemistry* **20**, 1269-1277.
- Boissy, G., O'Donohue, M., Gaubemer, O., Perez, B., Pernolet, J-P., and Brunie, S. (1999) *Protein Sci.* **8**, 1191-1199.
- Bouvier-nave, P., Husselstein, T., and Benveniste, P. (1998) *Eur. J. Biochem.* **256**, 88-96.
- Bradford, M.M. (1976) *Anal. Biochem.* **72**, 248-254.
- Copeland, R.A. *Enzymes: A Practical Introduction to Structure, Mechanism, and Data Analysis*. New York: Wiley-VCH Inc. Publications, 2000.
- Copeland, R.A. *Methods for Protein Analysis*. New York: International Thomson Publishing, 1994.
- Cornforth, J.W. (1968) *Agnew. Chem. Int. Ed. Engl.* **7**, 903-911.
- Dougherty, D.A. (1996) *Science* **271**, 163-168.
- Fu, Z., Hu, Y., Konishi, K., Takata, Y., Ogawa, H., Gomi, T., Fujioka, M., and Takusagawa, F. (1996) *Biochemistry* **35**, 11985-11993.
- Guo, D., Jia, Z., and Nes, W.D. (1996) *Tetrahedron Lett.* **37**, 6823-6826.
- Julia, H., and Marazano, C. (1985) *Tetrahedron* **41**, 3717-3724.
- Laemmli, U.K. (1970) *Nature* **227**, 680-685.
- Le, P.H., and Nes, W.D. (1986) *Chemistry and Physics of Lipids* **246**, 57-69.
- Kagan, R.M., and Clarke, S. (1994) *Arch. Biochem. Biophys.* **310**, 417-427.
- Malhotra, H.C., and Nes, W.R. (1971) *J. Biol. Chem.* **246**, 4934-4937.
- Marshall, J.A. (1998) Master's Thesis, Texas Tech University, 1-50.

- Marshall, J.A., and Nes, W.D. "ATP is an allosteric modulator of sterol C-methyltransferase activity" FASEB abstract for meeting on Biological Methylation Reactions, Saxtons Rivers, VT, July 1999.
- Marshall, J.A., and Nes, W.D. (1999) *Bioorganic & Med. Chem. Lett.* **9**, 1533-1536.
- Nes, W.D. (2000) *Biochim. Biophys. Acta* **55711**, 1-26.
- Nes, W.D., Guo, D., and Zhou, W. (1997) *Arch. Biochem. Biophys.* **341**, 68-81.
- Nes, W.D., McCourt, B.S., Marshall, J.A., Ma, J., Dennis, A.L., Lopez, M., Li, H., and Le,H. (1999) *J. Org. Chem.* **64**, 1535-1542.
- Nes, W.D., McCourt, B.S., Zhou, W-x., Ma, J., Marshall, J.A., Peek, L-A., and Brennan, M.(1998) *Arch. Biochem. Biophys.* **353**, 297-311.
- Nes, W.R., and McKean, M.L. *Biochemistry of steroids and other isopentenoids.* (1977), University Park Press, Baltimore, pp. 244-359.
- Niewmierzycka, A., and Clarke, S. (1999) *J. Biol. Chem.* **274**, 814-824.
- Parker, S.R., and Nes, W.D. "Regulation of sterol biosynthesis and its phylogenetic importance" (1992) *ACS Symp. Ser.* **497**, 110-145.
- Rahier, A., Genot, J-C., Schuber, F., Benveniste, P., and Narula, A.S. (1984) *J. Biol. Chem.* **259**, 15215-15223.
- Rose, A. *The Yeasts.* (1969) London: Academic Press.
- Roth, M., Helm-Kruse, S., Friedrich, T., and Jeltsch, A. (1998) *J. Biol.Chem.* **273**, 17333-17342.
- Subbaramaiah, K., and Simms, S.A. (1992) *J. Biol. Chem.* **267**, 8636-8642.
- Takata, Y., Konishi, K. Gomi, T., and Fujioka, M. (1994) *J. Biol. Chem.* **269**, 5537-5542.
- Venkatramesh, M., Guo, D., Harman, J.G., and Nes, W.D. (1996) *Lipids* **31**, 373-377.
- Venkatramesh, M., Guo, D., Jia, Z., and Nes, W.D. (1996) *Biochim. Biophys. Acta* **1299**, 313-324.
- West, C.A., Dudley, M.R., and Dueber, M.T. (1979) *Rec.Adv. Phytochem.* **13**, 163-198.
- Zhou, W-x. (1998) Master's Thesis, Texas Tech University, 1-83.

Zisner, E , Paltauf, F., and Daum, G. (1993) *J. Bacteriol.* **175**, 2853-2856.